

# A FAST AND SPECTRALLY CONVERGENT ALGORITHM FOR FRACTIONAL INTEGRAL AND DIFFERENTIAL EQUATIONS WITH HALF-INTEGER ORDER TERMS

NICHOLAS HALE \* AND SHEEHAN OLVER †

**Abstract.** A fast algorithm (linear in the degrees of freedom) for the solution of linear fractional integral and differential equations of half-integer order with variable coefficients is described. The approach is related to the ultraspherical method for ODEs [27], and involves constructing two different bases — one for the domain of the operator and one for the range of the operator — so that the operators are banded. The bases are constructed from direct sums of suitably weighted ultraspherical polynomial expansions for which explicit representations of fractional integrals and derivatives are derived. Spectral convergence is demonstrated when the variable coefficients and right-hand side are sufficiently smooth.

**Key words.** Fractional derivative, spectral method, Legendre polynomials, Chebyshev polynomials, Ultraspherical polynomials, Riemann–Liouville, Caputo, Bagley–Torvik

**AMS subject classifications.** 26A33, 34A08, 65L99

**1. Introduction.** Fractional derivatives and fractional differential equations (FDEs) are becoming increasingly prevalent in the mathematical modelling of biological and physical processes [11, 18, 21, 22, 24, 29, 31–33]. The typical numerical techniques for computing solutions are finite difference [10, 23, 40] or finite element-based [12, 15, 20], but these usually provide only low accuracy solutions due to the global nature of fractional derivatives. There have been some recent developments in spectral methods for FDEs [8, 19, 41], but these are only observed to achieve spectral accuracy for special solutions.

This paper concerns the numerical solution of linear equations involving half-integer order fractional integrals and derivatives on the interval  $[-1, 1]$ .<sup>1</sup> The (left-sided) half-integral is defined as [30]<sup>2</sup>

$${}_{-1}\mathcal{Q}_x^{1/2}f(x) = \frac{1}{\sqrt{\pi}} \int_{-1}^x \frac{f(t)}{(x-t)^{1/2}} dt, \quad (1.1)$$

and for  $m \in \mathbb{N}$ , we consider  $(m+1/2)$ -order derivatives of *Riemann–Liouville* (RL) and *Caputo* types,

$${}^{RL}\mathcal{D}_x^{m+1/2}f(x) = \frac{d^{m+1}}{dx^{m+1}} ({}_{-1}\mathcal{Q}_x^{1/2}f(x)) \quad \text{and} \quad {}^C\mathcal{D}_x^{m+1/2}f(x) = {}_{-1}\mathcal{Q}_x^{1/2} \left( \frac{d^{m+1}}{dx^{m+1}} f(x) \right). \quad (1.2)$$

We propose an approach that achieves spectral convergence in linear complexity for a broad class of linear fractional integral equations (FIEs) and FDEs composed of such half-integer order operators.

The proposed approach is related to the ultraspherical spectral (US) method for ordinary differential equations [27] and singular integral equations [34], where the key idea is that the underlying operators are banded when represented by their action on appropriately chosen bases, built out of ultraspherical polynomials. Here, for integral equations of the first kind, the idea is similar: we exploit the fact that fractional integration is a banded operator between two *weighted* ultraspherical polynomial bases, for which an explicit representation of the fractional derivative is available. However, a critical difficulty arises for integral equations of the second kind and differential equations: the bases are not compatible, in the sense that the weights in the range of the operators differ from those of the domain. To overcome this difficulty we consider the operators as acting on a basis formed as a direct sum of two weighted ultraspherical polynomial bases (namely Legendre and Chebyshev polynomials) and to represent the range of the operator we use another basis formed as a direct sum of two different weighted ultraspherical polynomial bases (for a total of four bases).

\*Department of Mathematical Sciences, Stellenbosch University, Stellenbosch, 7600, South Africa. (nickhale@sun.ac.za)

†School of Mathematics and Statistics, The University of Sydney, NSW 2006, Australia. (Sheehan.Olver@sydney.edu.au)

<sup>1</sup>Problems defined on any other bounded interval may be mapped to  $[-1, 1]$  by a suitable affine transformation.

<sup>2</sup>The right-sided half-integral,  ${}_x\mathcal{Q}_1^{1/2}$ , is similar, but with the limits on the integral changed from  $[-1, x]$  to  $[x, 1]$  and the bracketed term in the denominator of the integrand negated. Without loss of generality, we focus on the left-sided case.

There have been two recent additions to the literature which also provide spectral accuracy for FDEs, namely the works of Zayernouri and Karniadakis [41] and Chen, Shen, and Wang [8].<sup>3</sup> The foundation of both is the same formula for the fractional integral of weighted Jacobi polynomials (i.e., [3, Theorem 6.72(b)]) which we use to derive a relationship for the half-integral of weighted ultraspherical polynomials in Theorem 2.1 below. Whereas in this paper we limit our attention to half-integer order derivatives, both [8] and [41] deal with arbitrary orders, and so are in a sense more general. However, the algorithm proposed by Zayernouri and Karniadakis is collocation based, leading to dense matrices and  $\mathcal{O}(N^3)$  complexity. Spectral accuracy is demonstrated for a few select problems, but it is typically sub-geometric. Furthermore, the discussion is limited to zero Dirichlet boundary conditions. The algorithm of Chen, Shen, and Wang has linear complexity, but applies only to FDEs of the form  ${}_{-1}\mathcal{D}_x^\nu u(x) = f(x)$  and  ${}_x\mathcal{D}_1^\nu u(x) = f(x)$  (for both RL and Caputo definitions). In this work we shall consider FDEs which are linear combinations of half-integer order derivatives with more general boundary conditions and demonstrate *geometric* convergence with *linear* complexity.

The outline of this paper is as follows. In Section 2 we introduce some necessary preliminaries regarding ultraspherical polynomials, in particular an explicit formula for their fractional integrals and various transformations between different weighted ultraspherical polynomial expansions. In Sections 3–5 we use these to derive a fast and exponentially convergent algorithm for a certain class of half-integer order fractional integral and differential equations of Riemann–Liouville and Caputo type, respectively. Section 6 discusses some computational issues relating to these algorithms, such as the efficient computation of the required polynomial coefficients and solution of the linear systems describing the FIEs/FDEs. We conclude in Section 7 with one final example and some suggestions for future work.

**Remark:** The experiments in the paper were conducted in MATLAB (code to reproduce all figures is available at [16]), and a Julia implementation of the algorithm is available in ApproxFun.jl [26].

## 2. Preliminaries.

**2.1. Ultraspherical polynomials.** Our primary tools in this paper are the ultraspherical (or Gegenbauer) polynomials,  $C_n^{(\lambda)}(x)$ , orthogonal with respect to the weight function  $(1-x^2)^{\lambda-1/2}$  on the interval  $[-1, 1]$ . For any  $\lambda > 0$  the degree  $n$  ultraspherical polynomial may be defined via the recurrence [13, 18.9.1]

$$C_{-1}^{(\lambda)}(x) = 0, \quad C_0^{(\lambda)}(x) = 1, \quad (n+1)C_{n+1}^{(\lambda)}(x) = 2(n+\lambda)x C_n^{(\lambda)}(x) - (n+2\lambda-1)C_{n-1}^{(\lambda)}(x). \quad (2.1)$$

The Legendre polynomials,  $P_n(x)$ , and the second-kind Chebyshev polynomials,  $U_n(x)$ , are special cases of the ultraspherical polynomials with  $\lambda = \frac{1}{2}$  and  $\lambda = 1$ , respectively. These two will be of particular importance in our algorithms described in Sections 3–5.

For any  $x \in \mathbb{C}$ ,  $\lambda > 0$ , and  $\gamma \in \mathbb{R}$ , we define  $\mathbf{C}_\gamma^{(\lambda)}(x)$  as the quasimatrix — a ‘matrix’ whose ‘columns’ are functions defined on an interval. See [35]. — whose  $j$ th column is the degree  $(j-1)$ th ultraspherical polynomial with parameter  $\lambda$  weighted by  $(1+x)^\gamma$ , i.e.,

$$\mathbf{C}_\gamma^{(\lambda)}(x) := \left[ (1+x)^\gamma C_0^{(\lambda)}(x), (1+x)^\gamma C_1^{(\lambda)}(x), \dots \right]. \quad (2.2)$$

We refer to these as *weighted* ultraspherical bases and note that the columns of  $\mathbf{C}_\gamma^{(\lambda)}(x)$  are related to the “generalised Jacobi functions” of [8] and “polyfractinomials” of [41]. With each such basis (2.2) we may associate a space of coefficients,  $\mathbf{C}_\gamma^{(\lambda)} \cong \mathbb{C}^\infty$ , and if  $\underline{v} = (v_0, v_1, \dots)^\top \in \mathbf{C}_\gamma^{(\lambda)}$  such that

$$\sum_{k=0}^{\infty} |v_k| \sup_{-1 \leq x \leq 1} |C_k^{(\lambda)}(x)| = \sum_{k=0}^{\infty} |v_k| \frac{\Gamma(2\lambda+k)}{\Gamma(2\lambda)k!} < \infty, \quad (2.3)$$

then  $\mathbf{C}_\gamma^{(\lambda)}(x)\underline{v}$  defines a continuous function away from  $x = -1$ . For convenience, we denote  $\mathbf{P}_\gamma := \mathbf{C}_\gamma^{(1/2)}$ ,  $\mathbf{U}_\gamma := \mathbf{C}_\gamma^{(1)}$ , and  $\mathbf{C}^{(\lambda)} := \mathbf{C}_0^{(\lambda)}$ .

<sup>3</sup>There has also been recent work in spectral methods for *tempered* fractional differential equations (see, for example, [42]), but it is not clear that these approaches provide spectral accuracy in the limit  $\alpha \rightarrow 0$ , i.e., the non-tempered case.

Linear operators which can be applied to one such weighted ultraspherical basis and expanded in another induce infinite-dimensional matrices that can be viewed as acting between different  $\mathbf{C}_\gamma^{(\lambda)}$  spaces. For example, given a continuous linear operator  $\mathcal{L} : X \rightarrow Y$  so that  $(1+x)^\lambda C_k^{(\lambda)} \in X$  and  $(1+x)^c C_j^{(\ell)} \in Y$  with the property

$$\mathcal{L}[(1+\diamond)^\gamma C_k^{(\lambda)}](x) = \sum_{j=k-m}^{k+m} L_{jk} (1+x)^c C_j^{(\ell)}(x), \quad (2.4)$$

we can associate it with an  $m$ -banded (i.e., banded with bandwidth  $m$ ) infinite-dimensional matrix

$$L := \begin{pmatrix} L_{00} & \cdots & L_{0m} & & \\ \vdots & \ddots & L_{1m} & L_{1,m+1} & \\ L_{m0} & L_{m1} & \ddots & L_{mm} & \ddots \\ & L_{m+1,1} & \ddots & \ddots & \ddots \\ & & \ddots & \ddots & \ddots \end{pmatrix}. \quad (2.5)$$

Since  $L$  is banded, multiplication is a well-defined operation on  $\mathbb{C}^\infty$  and (2.5) can be viewed as an operator  $L : \mathbf{C}_\gamma^{(\lambda)} \rightarrow \mathbf{C}_c^{(\ell)}$ . To relate the operator  $L$  and the operator  $\mathcal{L}$  we note that, by construction, we have

$$\mathcal{L}[(1+\diamond)^\gamma C_k^{(\lambda)}](x) = \mathcal{L} \mathbf{C}_\gamma^{(\lambda)}(x) \underline{e}_k = \mathbf{C}_c^{(\ell)}(x) L \underline{e}_k. \quad (2.6)$$

Assuming that  $\mathbf{C}_\gamma^{(\lambda)}(x) \underline{e}_k$  are dense in  $X$ , then if  $v \in X$  there exists  $\underline{v}$  so that  $\mathbf{C}_\gamma^{(\lambda)}(x) \underline{v} = v$ . Because  $\mathcal{L}$  is continuous, we have

$$\mathcal{L}v = \mathcal{L} \mathbf{C}_\gamma^{(\lambda)}(x) \underline{v} = \mathbf{C}_c^{(\ell)}(x) L \underline{v}, \quad (2.7)$$

and therefore applying  $L$  to  $v$  is equivalent to applying  $\mathcal{L}$  to  $\underline{v}$ .

The US method [27] for differential equations requires three such banded operators which act on ultraspherical polynomials: conversion, multiplication, and differentiation. We now revisit these operators in the case of weighted ultraspherical polynomials and introduce new operators corresponding to fractional integration and fractional differentiation of half-integer order.

**Remark:** In Sections 3–5 we will seek solutions to FIEs and FDEs formed as linear combinations of Legendre polynomials,  $P_n(x)$ , and weighted Chebyshev polynomials of the second kind,  $\sqrt{1+x}U_n(x)$ . Another possibility is to choose a direct sum of Legendre polynomials and weighted Chebyshev polynomials of the *first* kind,  $T_n(x)/\sqrt{1+x}$  (for which one can also find explicit and compact formulae for half-integer order integrals and derivatives). We make the decision to use second-kind polynomials for the following reasons: Firstly,  $T_n(x)$  is not an ultraspherical polynomial. In particular, this means that the formulae involving  $T_n(x)$  in the next few sections must be treated separately from  $C^{(\lambda)}(x)$ , which great clutters the exposition. Secondly, in most applications of interest the solution remains finite, so a basis which remains bounded in the computational interval is preferred. Yet another possibility is work with more general Jacobi polynomials of appropriate degree and weighting, but again the formulae which follow are less elegant in this setting, and we prefer the ultraspherical polynomials for clarity of exposition.

**2.2. Conversion operators.** We consider two representations of the identity operator,  $\mathcal{I}$ , which map between different  $\mathbf{C}_\gamma^{(\lambda)}$  spaces. First, the relationship [13, 18.9.7]

$$C_n^{(\lambda)}(x) = \frac{\lambda}{n+\lambda} (C_n^{(\lambda+1)}(x) - C_{n-2}^{(\lambda+1)}(x)), \quad (2.8)$$

induces operators  $S_\lambda : \mathbf{C}_\gamma^{(\lambda)} \rightarrow \mathbf{C}_\gamma^{(\lambda+1)}$  defined by

$$S_\lambda := \begin{pmatrix} 1 & 0 & \frac{-\lambda}{\lambda+2} & & \\ & \frac{\lambda}{\lambda+1} & 0 & \frac{-\lambda}{\lambda+3} & \\ & & \frac{\lambda}{\lambda+2} & 0 & \frac{-\lambda}{\lambda+4} \\ & & & \ddots & \ddots \\ & & & & \ddots \end{pmatrix}. \quad (2.9)$$

These are precisely the conversion operators  $\mathcal{S}_\lambda$  as described in [27]. Here, and in the other operators that follow, when  $S$  is acting on either  $\mathbf{P}$  or  $\mathbf{U}$ , we shall subscript with these, rather than the corresponding value of  $\lambda$ . That is,

$$S_{\mathbf{P}} := S_{1/2} = \begin{pmatrix} 1 & 0 & -\frac{1}{5} & & \\ & \frac{1}{3} & 0 & -\frac{1}{7} & \\ & & \frac{1}{5} & 0 & \ddots \\ & & & \ddots & \ddots \end{pmatrix} \quad \text{and} \quad S_{\mathbf{U}} := S_1 = \begin{pmatrix} 1 & 0 & -\frac{1}{3} & & \\ & \frac{1}{2} & 0 & -\frac{1}{4} & \\ & & \frac{1}{3} & 0 & \ddots \\ & & & \ddots & \ddots \end{pmatrix}. \quad (2.10)$$

A second relationship

$$(1+x)C_n^{(\lambda)}(x) = \frac{n+1}{2(n+\lambda)}C_{n+1}^{(\lambda)}(x) + C_n^{(\lambda)}(x) + \frac{n+2\lambda-1}{2(n+\lambda)}C_{n-1}^{(\lambda)}(x), \quad \lambda > 0, \quad (2.11)$$

which can be readily derived from the recurrence relations (2.1), induces operators  $R_\lambda : \mathbf{C}_\gamma^{(\lambda)} \rightarrow \mathbf{C}_{\gamma-1}^{(\lambda)}$ , where

$$R_\lambda := \frac{1}{2} \begin{pmatrix} 2 & \frac{2\lambda}{1+\lambda} & & & \\ \frac{1}{\lambda} & 2 & \frac{1+2\lambda}{2+\lambda} & & \\ & \frac{2}{1+\lambda} & 2 & \frac{2+2\lambda}{3+\lambda} & \\ & & \frac{3}{2+\lambda} & 2 & \ddots \\ & & & \ddots & \ddots \end{pmatrix}. \quad (2.12)$$

Note that in particular  $R_{\mathbf{U}}$  has the simple form

$$R_{\mathbf{U}} := R_1 = \frac{1}{2} \begin{pmatrix} 2 & 1 & & \\ 1 & 2 & \ddots & \\ & \ddots & \ddots & \end{pmatrix}. \quad (2.13)$$

**2.3. Multiplication operators.** As outlined in [34] and [38], polynomial multiplication can be viewed as a banded operator acting on  $\mathbf{C}^{(\lambda)}$  spaces. In particular, the basic building block is the Jacobi operator, built out of the three-term recurrence (2.1):

$$xC_n^{(\lambda)}(x) = \frac{n+1}{2(n+\lambda)}C_{n+1}^{(\lambda)}(x) + \frac{n+2\lambda-1}{2(n+\lambda)}C_{n-1}^{(\lambda)}(x). \quad (2.14)$$

In the language of Section 2.1, this amounts to choosing  $\mathcal{L} = x$ , inducing the operator  $J_\lambda : \mathbf{C}_\gamma^{(\lambda)} \rightarrow \mathbf{C}_\gamma^{(\lambda)}$  defined as

$$J_\lambda := \frac{1}{2} \begin{pmatrix} 0 & \frac{2\lambda}{1+\lambda} & & & \\ \frac{1}{\lambda} & 0 & \frac{1+2\lambda}{2+\lambda} & & \\ & \frac{2}{1+\lambda} & 0 & \frac{2+2\lambda}{3+\lambda} & \\ & & \frac{3}{2+\lambda} & 0 & \ddots \\ & & & \ddots & \ddots \end{pmatrix}. \quad (2.15)$$

If  $C_n^{(\ell)}(x)$  is another ultraspherical polynomial then its corresponding three-term recurrence applied to  $J_\lambda$  gives

$$C_{n+1}^{(\ell)}(J_\lambda) = 2\frac{n+\ell}{n+1}J_\lambda C_n^{(\ell)}(J_\lambda) - \frac{n+2\ell-1}{n+1}C_{n-1}^{(\ell)}(J_\lambda), \quad (2.16)$$

and the multiplication operator  $\Pi_\lambda[C_n^{(\ell)}] : \mathbf{C}_\gamma^{(\lambda)} \rightarrow \mathbf{C}_\gamma^{(\lambda)}$  may be defined recursively as

$$\Pi_\lambda[C_{n+1}^{(\ell)}] = 2\frac{n+\ell}{n+1}J_\lambda \Pi_\lambda[C_n^{(\ell)}] - \frac{n+2\ell-1}{n+1}\Pi_\lambda[C_{n-1}^{(\ell)}], \quad (2.17)$$

where  $\Pi_\lambda[C_{-1}^{(\ell)}] = 0$  and  $\Pi_\lambda[C_0^{(\ell)}] = I$ . Each term in the recursion will increase by the bandwidth by 1 (since  $J_\lambda$  has bandwidth 1), so  $\Pi_\lambda[C_d^{(\ell)}]$  is banded with bandwidth  $d$ . Then, by linearity of  $\Pi_\lambda$  and the orthogonality of ultraspherical polynomials, given any degree  $d$  polynomial  $p$  we may construct

$$\Pi_\lambda\left[p(x) = \sum_{n=0}^d p_n C_n^{(\ell)}(x)\right] = \sum_{n=0}^d p_n \Pi_\lambda[C_n^{(\ell)}], \quad (2.18)$$

which also has bandwidth  $d$ .

For convenience and ease of notation we take  $\ell = \lambda$ , in which case the columns of  $\Pi_\lambda[C_d^{(\lambda)}]$  give rise to linearisation formulae for products of the form  $C_d^{(\lambda)}(x)C_n^{(\lambda)}(x)$  (see [13, 18.18.22]). When  $p$  is not a polynomial but a sufficiently differentiable function, we can approximate it to high accuracy by a polynomial. In particular, if  $p$  is analytic in some neighbourhood of  $[-1, 1]$ , then the polynomial approximation will converge geometrically, and the degree of the approximant (and hence bandwidth of  $\Pi_\lambda$ ) will typically be small.

**2.4. Integral operators.** The foundation of our approach is the following formula, which shows how the half-integral of certain weighted ultraspherical polynomials may be computed in closed form:

THEOREM 2.1. *For any  $\lambda > 0, n \geq 0$ ,*

$$_{-1}\mathcal{Q}_x^{1/2}[(1+x)^{\lambda-1/2}C_n^{(\lambda)}(x)] = \frac{\Gamma(\lambda+1/2)}{\Gamma(\lambda)(n+\lambda)}(1+x)^\lambda(C_n^{(\lambda+1/2)}(x) - C_{n-1}^{(\lambda+1/2)}(x)), \quad (2.19)$$

*Proof.* Follows from relating  $C_n^{(\lambda)}(x)$  to the Jacobi polynomial  $P_n^{(\lambda-1/2, \lambda-1/2)}(x)$  and using the closed form expression for fractional integrals of weighted Jacobi polynomials [3, Theorem 6.72(b)]. Applying the symmetric version of [13, 18.9.5] to the right-hand side and converting  $P_n^{(\lambda, \lambda)}(x)$  back to  $C_n^{(\lambda+1/2)}(x)$  yields the required result.  $\square$

COROLLARY 2.2.

$$_{-1}\mathcal{Q}_x^{1/2}P_n(x) = \frac{2\sqrt{1+x}}{\sqrt{\pi}(2n+1)}(U_n(x) - U_{n-1}(x)) \quad (2.20)$$

and

$$_{-1}\mathcal{Q}_x^{1/2}\sqrt{1+x}U_n(x) = \frac{\sqrt{\pi}}{2}(P_{n+1}(x) + P_n(x)) \quad (2.21)$$

*Proof.* The first follows immediately from setting  $\lambda = 1/2$  in (2.19). For the second, take  $\lambda = 1$  in (2.19) and make the observation (see Appendix A) that  $n(P_n(x) + P_{n-1}(x)) = (1+x)(C_{n-1}^{(3/2)}(x) - C_{n-2}^{(3/2)}(x))$ .  $\square$

We may therefore, in the language of Section 2.1, consider half-integration as a banded operator between the spaces of Legendre polynomials and weighted Chebyshev polynomials, and define the associated banded infinite dimensional matrices  $Q_{\mathbf{P}}^{1/2} : \mathbf{P} \rightarrow \mathbf{U}_{1/2}$  and  $Q_{\mathbf{U}_{1/2}}^{1/2} : \mathbf{U}_{1/2} \rightarrow \mathbf{P}$  as

$$Q_{\mathbf{P}}^{1/2} := \frac{2}{\sqrt{\pi}} \begin{pmatrix} 1 & -\frac{1}{3} & & \\ & \frac{1}{3} & -\frac{1}{5} & \\ & & \ddots & \ddots \end{pmatrix} \quad \text{and} \quad Q_{\mathbf{U}_{1/2}}^{1/2} := \frac{\sqrt{\pi}}{2} \begin{pmatrix} 1 & & & \\ 1 & 1 & & \\ & 1 & 1 & \\ & & \ddots & \ddots \end{pmatrix}, \quad (2.22)$$

respectively.

If we define  $Q_{\mathbf{P}} := Q_{\mathbf{U}_{1/2}}^{1/2} Q_{\mathbf{P}}^{1/2}$  so  $Q_{\mathbf{P}} : \mathbf{P} \rightarrow \mathbf{P}$  is given by

$$Q_{\mathbf{P}} = \begin{pmatrix} 1 & -\frac{1}{3} & & \\ 1 & 0 & -\frac{1}{5} & \\ & \frac{1}{3} & 0 & -\frac{1}{7} \\ & & \frac{1}{5} & 0 & \ddots \\ & & & \ddots & \ddots \end{pmatrix}, \quad (2.23)$$

we see that this is consistent with the relation

$${}_{-1}\mathcal{Q}_x^1 P_n(x) = \int_{-1}^x P_n(t) dt = \begin{cases} \frac{1}{2n+1}(P_n(x) - P_{n-2}(x)), & n \geq 1, \\ P_1(x) + P_0(x), & n = 0, \end{cases} \quad (2.24)$$

for the integral of Legendre polynomials (which can be obtained from [13, 18.16.1] and [13, 18.9.6]). We may go farther and repeatedly combine the  $Q_{\mathbf{P}}$  and  $Q_{\mathbf{U}_{1/2}}$  operators to define banded operators  $Q_{\mathbf{P}}^{m+1/2}$  and  $Q_{\mathbf{U}_{1/2}}^{m+1/2}$  between the spaces  $\mathbf{P}$  and  $\mathbf{U}_{1/2}$  representing integral operators of half-integer order, i.e.,  ${}_{-1}\mathcal{Q}_x^{m+1/2}$ . In particular, we have

$$Q_{\mathbf{P}}^{m+1/2} := Q_{\mathbf{P}}^{1/2} (Q_{\mathbf{U}_{1/2}}^{1/2} Q_{\mathbf{P}}^{1/2})^m : \mathbf{P} \rightarrow \mathbf{U}_{1/2}, \quad (2.25)$$

and

$$Q_{\mathbf{U}_{1/2}}^{m+1/2} := Q_{\mathbf{U}_{1/2}}^{1/2} (Q_{\mathbf{P}}^{1/2} Q_{\mathbf{U}_{1/2}}^{1/2})^m : \mathbf{U}_{1/2} \rightarrow \mathbf{P}. \quad (2.26)$$

Integral operators of integer order,  $\mathcal{Q}^m$ , acting on these same spaces give rise to banded operators  $Q_{\mathbf{P}}^m : \mathbf{P} \rightarrow \mathbf{P}$  and  $Q_{\mathbf{U}_{1/2}}^m : \mathbf{U}_{1/2} \rightarrow \mathbf{U}_{1/2}$ , which can be constructed likewise by omitting the terms outside the parentheses in (2.25) and (2.26), respectively.

**Remark:** Both  $Q_{\mathbf{P}}^{m+1/2}$  and  $Q_{\mathbf{U}_{1/2}}^{m+1/2}$  have bandwidth  $m+1$ .

**2.5. Differentiation operators.** The final key ingredient for the US method for ordinary differential equations is the relationship

$$\frac{d}{dx} C_n^{(\lambda)}(x) = 2\lambda C_{n-1}^{(\lambda+1)}(x). \quad (2.27)$$

This induces banded operators  $D_\lambda : \mathbf{C}^\lambda \rightarrow \mathbf{C}^{\lambda+1}$ , and more generally  $D_\lambda^m : \mathbf{C}^\lambda \rightarrow \mathbf{C}^{\lambda+m}$ , defined by

$$D_\lambda := 2\lambda \begin{pmatrix} 0 & 1 & & \\ & & 1 & \\ & & & \ddots \end{pmatrix} \quad \text{and} \quad D_\lambda^m := 2^m \lambda^{(m)} \begin{pmatrix} \overbrace{0 \cdots 0}^{m \text{ times}} & & 1 & \\ & & & 1 & \\ & & & & \ddots \end{pmatrix}, \quad (2.28)$$

respectively (where  $\lambda^{(m)} = \lambda(\lambda+1)\dots(\lambda+m-1)$  is the Pochhammer function or “rising factorial”).

We now derive similar such operators for half-integer order derivatives of weighted ultraspherical polynomials. For now we consider only the Riemann–Liouville definition, for which we have that:

COROLLARY 2.3.

$${}_{-1}^{RL}\mathcal{D}_x^{1/2} P_n(x) = \frac{1}{\sqrt{\pi}\sqrt{1+x}} (U_n(x) + U_{n-1}(x)) \quad (2.29)$$

and

$${}_{-1}^{RL}\mathcal{D}_x^{1/2} \sqrt{1+x} U_n(x) = \frac{\sqrt{\pi}}{2} (C_n^{(3/2)}(x) + C_{n-1}^{(3/2)}(x)) \quad (2.30)$$

*Proof.* The second equation follows immediately from differentiating (2.21) in Corollary 2.2 using (2.27). For the first equation, differentiate the right-hand side of (2.21) via the product rule and make the observation (see Appendix A) that  $2(1+x)(C_{n-1}^{(2)}(x) - C_{n-2}^{(2)}(x)) = nU_n(x) + (n+1)U_{n-1}(x)$ .  $\square$

Therefore, similarly to the case of half-integrals above, we may consider half-differentiation as a banded operator acting on  $\mathbf{P}$  and  $\mathbf{U}_{1/2}$ , but now mapping to  $\mathbf{U}_{-1/2}$  and  $\mathbf{C}^{(3/2)}$ , respectively. In particular, we have  $D_{\mathbf{P}}^{1/2} : \mathbf{P} \rightarrow \mathbf{U}_{-1/2}$  and  $D_{\mathbf{U}_{1/2}}^{1/2} : \mathbf{U}_{1/2} \rightarrow \mathbf{C}^{(3/2)}$ , given by the banded infinite dimensional matrices

$$D_{\mathbf{P}}^{1/2} := \frac{1}{\sqrt{\pi}} \begin{pmatrix} 1 & 1 & & \\ & 1 & 1 & \\ & & & \ddots & \ddots \end{pmatrix} \quad \text{and} \quad D_{\mathbf{U}_{1/2}}^{1/2} := \frac{\sqrt{\pi}}{2} \begin{pmatrix} 1 & 1 & & \\ & 1 & 1 & \\ & & & \ddots & \ddots \end{pmatrix}. \quad (2.31)$$

Since the composition of these operators is no longer a mapping between the same space, we cannot construct higher-order derivatives in the same way we did higher-order integral operators. However, applying equation (2.27)  $m$  times to  $P_n(x)$  and (2.30), we may readily write

$$\frac{d^m}{dx^m} P_n(x) = 2^m \left(\frac{1}{2}\right)^{(m)} C_{n-m}^{(m+1/2)}(x) = \frac{2^m \Gamma(m+1/2)}{\sqrt{\pi}} C_{n-m}^{(m+1/2)}(x) \quad (2.32)$$

and

$${}^{RL}_{-1} \mathcal{D}_x^{m+1/2} \sqrt{1+x} U_n(x) = 2^m \Gamma(m+3/2) (C_{n-m}^{(m+3/2)}(x) + C_{n-m-1}^{(m+3/2)}(x)), \quad (2.33)$$

and can consider  $D_{\mathbf{P}}^m : \mathbf{P} \rightarrow \mathbf{C}^{(m+1/2)}$  and  $D_{\mathbf{U}_{1/2}}^{m+1/2} : \mathbf{U}_{1/2} \rightarrow \mathbf{C}^{(m+3/2)}$  defined by

$$D_{\mathbf{P}}^m := \frac{2^m \Gamma(m+1/2)}{\sqrt{\pi}} \begin{pmatrix} \overbrace{0 \dots 0}^{m \text{ times}} & 1 & & \\ & & 1 & \\ & & & \ddots \end{pmatrix} \text{ and } D_{\mathbf{U}_{1/2}}^{m+1/2} := 2^m \Gamma(m+3/2) \begin{pmatrix} \overbrace{0 \dots 0}^{m \text{ times}} & 1 & 1 & \\ & & 1 & \ddots \\ & & & \ddots \end{pmatrix}. \quad (2.34)$$

**Remark:** Observe that  $D_{\mathbf{P}}^m$  and  $D_{\mathbf{U}_{1/2}}^{m+1/2}$  are banded with bandwidths  $m$  and  $m+1$ , respectively.

The corresponding operators for  $\frac{d^m}{dx^m} \sqrt{1+x} U_n(x)$  and  ${}^{RL}_{-1} \mathcal{D}_x^{m+1/2} P_n(x)$  are complicated by the  $\sqrt{1+x}$  weights. Here we must appeal to the product rule for differentiation and derive recursive formulations for  $D_{\mathbf{U}_{1/2}}^m$  and  $D_{\mathbf{P}}^{m+1/2}$ . We first note that:

LEMMA 2.4. *For any  $n \geq 0, \lambda > 0, \mu \neq 0$*

$$\frac{d}{dx} (1+x)^\mu C_n^{(\lambda)}(x) = \lambda (1+x)^{\mu-1} \left[ \left(1 + \frac{\mu-\lambda}{n+\lambda}\right) C_n^{(\lambda+1)}(x) + 2C_{n-1}^{(\lambda+1)}(x) + \left(1 - \frac{\mu-\lambda}{n+\lambda}\right) C_{n-2}^{(\lambda+1)}(x) \right], \quad (2.35)$$

(where  $C_{-2}^{(\lambda+1)}(x) := 0$ ).

*Proof.* Apply the product rule to the left-hand side, then use (2.8), (2.11), and (2.27).  $\square$

If we define  $D_{\mu,\lambda} : \mathbf{C}_\mu^{(\lambda)} \rightarrow \mathbf{C}_{\mu-1}^{(\lambda+1)}$  as the operator induced by this relationship, i.e.,

$$D_{\mu,\lambda} := \lambda \begin{pmatrix} 1 & 2 & 1 & & \\ & 1 & 2 & 1 & \\ & & 1 & 2 & \ddots \\ & & & \ddots & \ddots \end{pmatrix} + \lambda(\mu-\lambda) \begin{pmatrix} \frac{1}{\lambda} & 0 & -\frac{1}{\lambda+2} & & \\ & \frac{1}{\lambda+1} & 0 & -\frac{1}{\lambda+3} & \\ & & \frac{1}{\lambda+2} & 0 & \ddots \\ & & & \ddots & \ddots \end{pmatrix} \quad (2.36)$$

we may then define  $D_{\mathbf{U}_{1/2}}^m : \mathbf{U}_{1/2} \rightarrow \mathbf{C}_{-m+1/2}^{(m+1)}$  and  $D_{\mathbf{P}}^{m+1/2} : \mathbf{P} \rightarrow \mathbf{C}_{-m-1/2}^{(m+1)}$  as

$$D_{\mathbf{U}_{1/2}}^m := \prod_{k=0}^{m-1} D_{-k+\frac{1}{2}, k+1} \quad \text{and} \quad D_{\mathbf{P}}^{m+1/2} := \left( \prod_{k=0}^{m-1} D_{-k-\frac{1}{2}, k+1} \right) D_{\mathbf{P}}^{1/2}, \quad (2.37)$$

respectively.

**Remark:** Since the  $D_{\mu,\lambda}$  operators each have bandwidth 2 (and recalling that  $D_{\mathbf{P}}^{1/2}$  has bandwidth 1), it is readily verified that  $D_{\mathbf{U}_{1/2}}^m$  and  $D_{\mathbf{P}}^{m+1/2}$  will have bandwidths  $2m$  and  $2m+1$ , respectively.

**2.6. Block operators.** As we shall see in the next section, our approach for solving FIEs and FDEs of half-integer order will be to seek solutions formed as a direct sum of two different weighted ultraspherical polynomials, namely  $\mathbf{P} \oplus \mathbf{U}_{1/2}$ . Here we introduce some notation to clarify the exposition in the description of the algorithm that follows. In particular, for any  $m \in \mathbb{N}$  we define

$$Q^{m/2} := \begin{pmatrix} 0 & Q_{\mathbf{U}_{1/2}}^{1/2} \\ Q_{\mathbf{P}}^{1/2} & 0 \end{pmatrix}^m : \mathbf{P} \oplus \mathbf{U}_{1/2} \rightarrow \mathbf{P} \oplus \mathbf{U}_{1/2}, \quad (2.38)$$

$$D^m := \begin{pmatrix} D_{\mathbf{P}}^m & 0 \\ 0 & D_{\mathbf{U}_{1/2}}^m \end{pmatrix} : \mathbf{P} \oplus \mathbf{U}_{1/2} \rightarrow \mathbf{C}^{(m+1/2)} \oplus \mathbf{C}_{-m+1/2}^{(m+1)}, \quad (2.39)$$

and

$$D^{m+1/2} := \begin{pmatrix} 0 & D_{\mathbf{U}}^{m+1/2} \\ D_{\mathbf{P}}^{m+1/2} & 0 \end{pmatrix} : \mathbf{P} \oplus \mathbf{U}_{1/2} \rightarrow \mathbf{C}^{(m+3/2)} \oplus \mathbf{C}_{-m-1/2}^{(m+1)}, \quad (2.40)$$

corresponding to half-integer order integral and derivative operators, respectively.

For convenience we also introduce the block conversion operators  $E_m : \mathbf{C}_{\gamma_1}^{(\ell)} \oplus \mathbf{C}_{\gamma_2}^{(m)} \rightarrow \mathbf{C}_{\gamma_1}^{(\ell)} \oplus \mathbf{C}_{\gamma_2}^{(m+1)}$  and  $E_{m+1/2} : \mathbf{C}_{\gamma_1}^{(m+1/2)} \oplus \mathbf{C}_{\gamma_2}^{(m+1)} \rightarrow \mathbf{C}_{\gamma_1}^{(m+3/2)} \oplus \mathbf{C}_{\gamma_2-1}^{(m+1)}$ ,  $m \in \mathbb{N}^+$  defined by

$$E_m := \begin{pmatrix} I & 0 \\ 0 & S_m \end{pmatrix} \quad \text{and} \quad E_{m+1/2} := \begin{pmatrix} S_{m+1/2} & 0 \\ 0 & R_{m+1} \end{pmatrix}. \quad (2.41)$$

**Remark:** Note that all of the operators in equations (2.38)–(2.41) are banded or block-banded. Block-banded matrices become banded when the coefficients are interleaved, which is expanded on below.

As described in Section 2.3, polynomial multiplication also results in banded operators. In particular, multiplication by a polynomial  $r(x) \in \mathbb{P}^d$  yields the following  $d$ -banded operator  $\Pi_0[r, 0] : \mathbf{P} \oplus \mathbf{U}_{1/2} \rightarrow \mathbf{P} \oplus \mathbf{U}_{1/2}$ ,

$$\Pi_0[r, 0] := \begin{pmatrix} \Pi_{\mathbf{P}}[r] & \\ & \Pi_{\mathbf{U}}[r] \end{pmatrix}. \quad (2.42)$$

More generally, for integer values  $m$ , we define multiplication operators

$$\Pi_m[r, 0] := \begin{pmatrix} \Pi_{m+1/2}[r] & \\ & \Pi_{m+1}[r] \end{pmatrix}, \quad \Pi_{m+1/2}[r, 0] := \begin{pmatrix} \Pi_{m+3/2}[r] & \\ & \Pi_{m+1}[r] \end{pmatrix}, \quad (2.43)$$

which act on the appropriate direct sum spaces.

Multiplication by square root-weighted polynomials,  $\sqrt{1+xs}(x)$ ,  $s \in \mathbb{P}^d$ , is complicated by the need to convert between  $\mathbf{C}^{(\lambda)}$  and  $\mathbf{C}^{(\lambda+1/2)}$  bases. For example, in the case of  $\sqrt{1+xs}(x)$  multiplying a vector in  $\mathbf{P} \oplus \mathbf{U}_{1/2}$  we require the upper triangular conversion or “connection” operators  $\hat{M} : \mathbf{P} \rightarrow \mathbf{U}$  and  $\hat{L} : \mathbf{U} \rightarrow \mathbf{P}$  [2,37] so that<sup>4</sup>

$$\Pi_0[0, s] := \begin{pmatrix} \hat{L}\Pi_{\mathbf{U}}[(1+\diamond)s] \\ \Pi_{\mathbf{U}}[s]\hat{M} \end{pmatrix}. \quad (2.44)$$

More generally, multiplication by  $r(x) + \sqrt{1+xs}(x)$  yields the operator  $\Pi_0[r, s] : \mathbf{P} \oplus \mathbf{U}_{1/2} \rightarrow \mathbf{P} \oplus \mathbf{U}_{1/2}$ ,

$$\Pi_0[r, s] := \begin{pmatrix} \Pi_{\mathbf{P}}[r] & \hat{L}\Pi_{\mathbf{U}}[(1+\diamond)s] \\ \Pi_{\mathbf{U}}[s]\hat{M} & \Pi_{\mathbf{U}}[r] \end{pmatrix}. \quad (2.45)$$

**Remark:**  $\Pi_0[0, s]$  and  $\Pi_0[r, s]$  are neither banded or block-banded, however they are (upon re-ordering) *lower*-banded. We give an example with such a weighted non-constant coefficient below, but will otherwise limit our attention to the case when the non-constant coefficients are smooth (i.e., well-approximated by an unweighted polynomial).

**3. Half-integer order integral equations.** We will now use the operators described above to derive an algorithm for integral equations of half-integer order.

<sup>4</sup>We use  $\hat{L}$  and  $\hat{M}$  here as  $L$  and  $M$  are typically used to denote the conversion operators  $M : \mathbf{P} \rightarrow \mathbf{T}$  and  $L : \mathbf{T} \rightarrow \mathbf{P}$ , respectively, where  $\mathbf{T}$  is the quasimatrix whose columns are formed of Chebyshev polynomials of the first kind,  $T_n(x)$ .



**3.1. Half-integral Equations.** Let's first consider Abel-like integral equations of the form

$$\sigma u(x) + {}_{-1}\mathcal{Q}_x^{1/2}u(x) = e(x) + \sqrt{1+x}f(x), \quad x \in [-1, 1], \quad (3.1)$$

where  $e(x)$  and  $f(x)$  are smooth (typically analytic in some neighbourhood of  $[-1, 1]$ ) and  $\sigma > 0$ .

We make the ansatz that the solution  $u(x)$  may be expressed as a linear combination of Legendre polynomials and weighted Chebyshev polynomials:

$$u(x) = \sum_{n=0}^{\infty} a_n P_n(x) + \sqrt{1+x} \sum_{n=0}^{\infty} b_n U_n(x). \quad (3.2)$$

(Formally this direct sum-space defines a frame [9]. We discuss this further in the Sections B.1 and 6.1.) Assuming the coefficients  $a_0, a_1, \dots$  and  $b_0, b_1, \dots$  satisfy the conditions (2.3), we may, in the language of Section 2, write

$$u(x) = [\mathbf{P}(x), \mathbf{U}_{1/2}(x)] \begin{pmatrix} \underline{a} \\ \underline{b} \end{pmatrix}. \quad (3.3)$$

Applying the block half-integral operator for this direct sum-space from Section 2.6 we have that

$${}_{-1}\mathcal{Q}_x^{1/2}u(x) = [\mathbf{P}(x), \mathbf{U}_{1/2}(x)] Q^{1/2} \begin{pmatrix} \underline{a} \\ \underline{b} \end{pmatrix} \quad (3.4)$$

and hence

$$\sigma u(x) + {}_{-1}\mathcal{Q}_x^{1/2}u(x) = [\mathbf{P}(x), \mathbf{U}_{1/2}(x)] (\sigma I + Q^{1/2}) \begin{pmatrix} \underline{a} \\ \underline{b} \end{pmatrix}. \quad (3.5)$$

Letting

$$e(x) = \sum_{n=0}^{\infty} e_n P_n(x) \quad \text{and} \quad f(x) = \sum_{n=0}^{\infty} f_n U_n(x), \quad (3.6)$$

or equivalently

$$e(x) + \sqrt{1+x}f(x) = [\mathbf{P}(x), \mathbf{U}_{1/2}(x)] \begin{pmatrix} \underline{e} \\ \underline{f} \end{pmatrix}, \quad (3.7)$$

and equating coefficients, we arrive at the (infinite dimensional) linear system of equations

$$(\sigma I + Q^{1/2}) \begin{pmatrix} \underline{a} \\ \underline{b} \end{pmatrix} = \begin{pmatrix} \sigma I & Q_{\mathbf{U}_{1/2}}^{1/2} \\ Q_{\mathbf{P}}^{1/2} & \sigma I \end{pmatrix} \begin{pmatrix} \underline{a} \\ \underline{b} \end{pmatrix} = \begin{pmatrix} \underline{e} \\ \underline{f} \end{pmatrix}. \quad (3.8)$$

Note that both the diagonal and off-diagonal blocks of the operator in (3.8) are banded, and by interleaving the coefficients in  $\underline{a}$  and  $\underline{b}$  (i.e.,  $(\underline{a}^\top, \underline{b}^\top) \mapsto (a_0, b_0, a_1, b_1, \dots)^\top$ ) we arrive at a banded operator (in this case, tridiagonal). Taking a finite section approximation (i.e., truncating each of the summations in (3.2) and (3.6) and hence the block operators in (3.8)) at a suitable length  $N$ , we arrive at a  $2N \times 2N$  tridiagonal matrix system, which can be solved directly in  $\mathcal{O}(N)$  floating point operations for the approximate coefficients  $\underline{a}$  and  $\underline{b}$  of  $u(x)$  in (3.2). Alternatively, one can use the adaptive QR approach described in [27] and solve the infinite dimensional (3.8) system to a required accuracy without *a priori* truncation (see Section 6.2). Convergence and stability are discussed in more detail in Appendix B.

**Example 1:** We consider the second-kind Abel integral equation

$$u(x) + {}_{-1}\mathcal{Q}_x^{1/2}u(x) = 1 \quad (3.9)$$

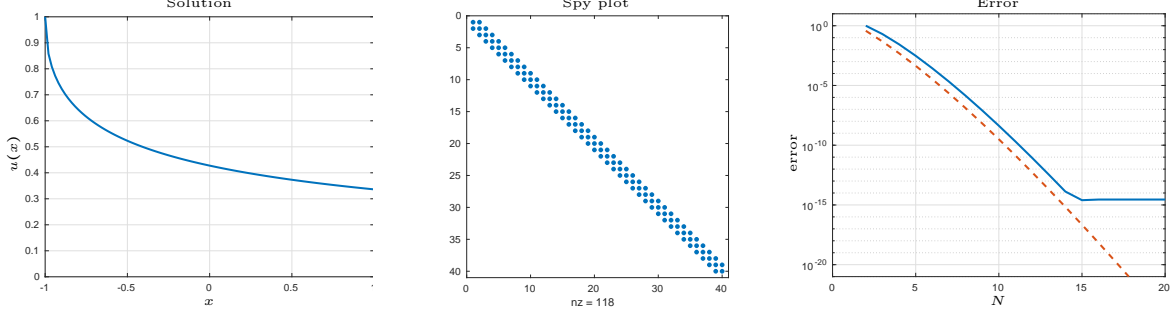


FIG. 3.1. (a) Approximate solution to (3.9) when  $N = 20$ . (b) MATLAB `spy` plot of (3.8) when  $N = 20$ . (c) Two measures of the error in the approximation as  $N$  varies. Solid line: Infinity norm error of solution approximated on a 100-point equally spaced grid. Dashed line: 2-norm difference between the coefficients of the approximated solution when truncating at sizes  $N$  and  $\lceil 1.1N \rceil$ .

(i.e., taking  $\sigma = 1$  in (3.1)) with solution [1]

$$u(x) = e^{1+x} \operatorname{erfc}(\sqrt{1+x}), \quad (3.10)$$

where  $\operatorname{erfc}$  is the complimentary error function. Note that the solution  $u(x)$  takes the form  $p(x) + \sqrt{1+x}q(x)$ , where  $p(x)$  and  $q(x)$  are functions analytic in some neighbourhood of  $[-1, 1]$ , and so any attempt to approximate  $u(x)$  by a polynomial  $y(x) \approx p_N(x)$  or a weighted polynomial  $u(x) \approx \sqrt{1+x}q_N(x)$  will achieve only algebraic convergence as the degree of the polynomial is increased. However, using the direct sum basis  $\mathbf{P} \oplus \mathbf{U}_{1/2}$  we are able to approximate such a function and hence solve the FDE (3.9) with geometrically accuracy.

To solve the FDE (3.9) we form the linear system (3.8) with  $\sigma = 1$ ,  $\underline{e} = (1, 0, \dots)^\top$ , and  $\underline{f} = (0, 0, \dots)^\top$ , truncate at some length  $N$ , and solve with `\` in MATLAB. The results are shown in Figure 3.1. The first image shows a plot of the computed solution with  $N = 20$ . The spy plot in the second image verifies that, upon re-ordering, the associated linear system (3.8) is tridiagonal. The third image shows two measures of the error in the approximation as  $N$  is increased.<sup>5</sup> The first (solid line) is computed by evaluating the approximate solution on a 100-point equally-spaced grid in the interval  $[-1, 1]$  using Clenshaw's algorithm and comparing to the true solution (3.10). Geometric convergence is observed until it plateaus at around 15 digits of accuracy when  $N = 15$ . The second measure (dashed line) is the 2-norm difference between the coefficients of the approximated solution when truncating at sizes  $N$  and  $\lceil 1.1N \rceil$ . Here the convergence does not plateau, suggesting that the computed coefficients maintain good relative accuracy even when their magnitude is below machine precision.

**3.2. Half-Order integral equations with non-constant coefficients.** In much the same way as in the US method for ODEs [27], the approach outlined above is readily extended to FDEs with non-constant coefficients. In particular, to solve problems of the form

$$u(x) + r(x) {}_{-1}\mathcal{Q}_x^{1/2} u(x) = e(x) + \sqrt{1+x} f(x). \quad (3.11)$$

we can appeal to the discussion in Section 2.3 and construct multiplication operators  $\Pi_{\mathbf{P}}[r]$  and  $\Pi_{\mathbf{U}}[r]$ , which act on Legendre and second-kind Chebyshev series, respectively. If  $r(x)$  is a polynomial of degree  $d$ , then these two operators will have bandwidth  $d$ . If  $r(x)$  is not a polynomial but is sufficiently smooth (for example, analytic), then the coefficients in its ultraspherical polynomial expansion will decay rapidly, and we may consider  $\Pi_{\mathbf{P}}[r]$  and  $\Pi_{\mathbf{U}}[r]$  as banded for practical purposes. The resulting linear system then takes the form

$$(I + \Pi_0[r, 0]Q^{1/2}) \begin{pmatrix} \frac{a}{b} \end{pmatrix} = \begin{pmatrix} \frac{e}{f} \end{pmatrix}, \quad (3.12)$$

<sup>5</sup>We show both measures here to validate the use of the second, which we employ later when a closed-form expression of the true solution is not readily available.

where  $\Pi_0[r, 0]$  is defined in Section 2.6.

We may also consider problems of the form

$$u(x) + {}_{-1}\mathcal{Q}_x^{1/2}[ru](x) = e(x) + \sqrt{1+x}f(x), \quad (3.13)$$

in which case the linear system becomes

$$(I + Q^{1/2}\Pi_0[r, 0]) \begin{pmatrix} \underline{a} \\ \underline{b} \end{pmatrix} = \begin{pmatrix} \underline{e} \\ \underline{f} \end{pmatrix}. \quad (3.14)$$

Similarly, problems of the form

$$u(x) + (r(x) + \sqrt{1+x}s(x)) {}_{-1}\mathcal{Q}_x^{1/2}u(x) = e(x) + \sqrt{1+x}f(x). \quad (3.15)$$

and

$$u(x) + {}_{-1}\mathcal{Q}_x^{1/2}[(r + \sqrt{1+x}s)u](x) = e(x) + \sqrt{1+x}f(x). \quad (3.16)$$

may also be solved with linear systems

$$(I + \Pi_0[r, s]Q^{1/2}) \begin{pmatrix} \underline{a} \\ \underline{b} \end{pmatrix} = \begin{pmatrix} \underline{e} \\ \underline{f} \end{pmatrix}, \quad (3.17)$$

and

$$(I + Q^{1/2}\Pi_0[r, s]) \begin{pmatrix} \underline{a} \\ \underline{b} \end{pmatrix} = \begin{pmatrix} \underline{e} \\ \underline{f} \end{pmatrix}, \quad (3.18)$$

respectively. However, these systems are no longer banded, and we will lose the linear complexity of our algorithm. Upon reordering they are dense above the diagonal and banded below, so Gaussian elimination will have quadratic complexity on the number of degrees of freedom.

**Example 2:** We adapt the example of Section 1 so that

$$u(x) + e^{-(1+x)/2} {}_{-1}\mathcal{Q}_x^{1/2}[e^{(1+x)/2}u](x) = e^{-(1+x)/2} \quad (3.19)$$

with solution

$$u(x) = e^{(1+x)/2} \operatorname{erfc}(\sqrt{1+x}). \quad (3.20)$$

Again taking  $u(x)$  as in (3.2), the resulting linear system defining the coefficients  $\underline{a}$  and  $\underline{b}$  is of the form

$$(I + \Pi[e^{-(1+x)/2}, 0]Q^{1/2}\Pi_0[e^{(1+x)/2}, 0]) \begin{pmatrix} \underline{a} \\ \underline{b} \end{pmatrix} = \begin{pmatrix} \underline{e} \\ \underline{0} \end{pmatrix}, \quad (3.21)$$

where  $\underline{e}$  are the Legendre coefficients of the function  $e^{-(1+x)/2}$ . (See Section 6.1 for discussion on how these are computed.) As in the previous example, we truncate each of the expansions at a suitable length  $N$  and solve the resulting finite dimensional banded matrix problem using `\` in MATLAB.

The results are shown in Figure 3.2. The left panel shows the approximate solution computed with  $N = 20$ . The centre panel shows a `spy` plot of the discretised, truncated, and re-ordered operator (3.21). The non-constant coefficients in equation (3.19) mean the resulting matrix is no longer tridiagonal, however, it is banded independently of  $N$  and can be solved by `\` in linear time as  $N \rightarrow \infty$ . The precise bandwidth depends on the number of Legendre coefficients required to approximate the non-constant coefficients, in this case  $e^{\pm(1+x)/2}$ , to machine precision accuracy. Here the number of coefficients required is around 14, and the resulting matrix has a bandwidth of approximately 43. The final panel shows the accuracy of the computed solution as  $N$  increases, using the same two forms of the error estimate as described in Example 1.

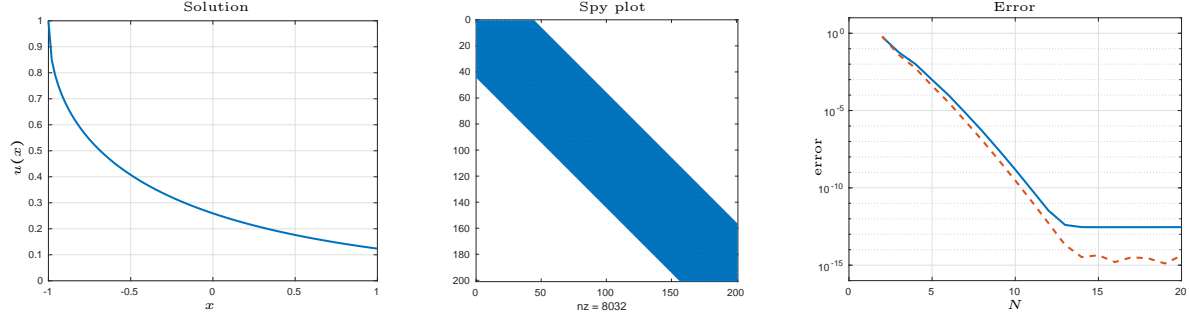


FIG. 3.2. (a) Approximate solution to (3.19) when  $N = 20$ . (b) MATLAB spy plot of (3.21) when  $N = 100$ . (c) Two measures of the error in the approximation as  $N$  varies. Solid line: Infinity norm error of solution approximated on a 100-point equally spaced grid. Dashed line: 2-norm difference between the coefficients of the approximated solution when truncating at sizes  $N$  and  $[1.1N]$ .

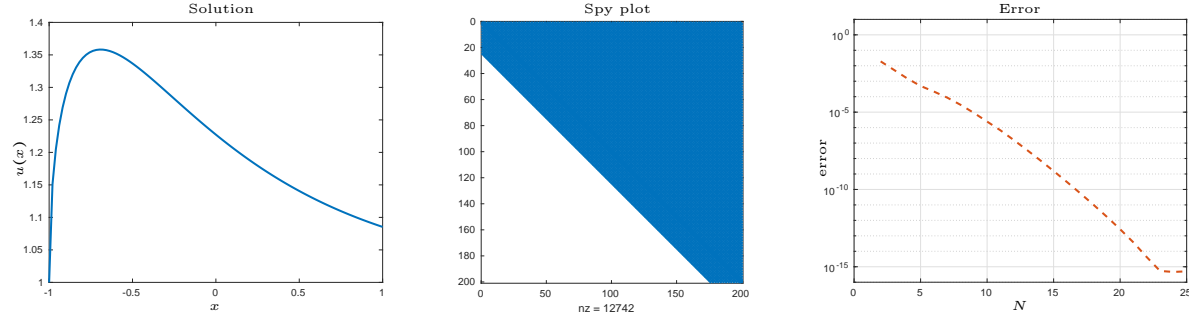


FIG. 3.3. (a) Approximate solution to (3.22) when  $N = 25$ . (b) MATLAB spy plot of (3.23) when  $N = 100$ . (c) 2-norm difference between the coefficients of the approximated solution when truncating at sizes  $N$  and  $[1.1N]$ .

Exponential convergence is again observed, but here both measures of the error plateau due to rounding error in the computation of the Chebyshev and/or Legendre coefficients of the functions  $e^{\pm(1+x)/2}$ .

**Example 3:** Here we solve

$$u(x) - \operatorname{erfc}\sqrt{1+x} {}_{-1}Q_x^{1/2} u(x) = 1. \quad (3.22)$$

The linear system we solve for the coefficients  $\underline{a}$  and  $\underline{b}$  is then of the form

$$\left( I + \Pi_0 \left[ -1, \frac{\operatorname{erf}(\sqrt{1+x})}{\sqrt{1+x}} \right] Q^{1/2} \right) \begin{pmatrix} \underline{a} \\ \underline{b} \end{pmatrix} = \begin{pmatrix} 1 \\ \underline{0} \end{pmatrix}. \quad (3.23)$$

Results are shown in Figure 3.3. Here, in the spy plot in the centre panel we see that as expected, the required change of bases  $\mathbf{P} \leftrightarrow \mathbf{U}_{1/2}$  are no longer banded, and hence neither is the re-ordered version of (3.23). However, the re-ordered matrix is *lower*-banded, and MATLAB's `\` will therefore require  $\mathcal{O}(N^2)$  operations to solve such systems directly via Gaussian elimination.

In this case we do not know an explicit for of the solution, and so in the right panel show only the accuracy estimate based upon comparison of successive approximations. We again observe geometric convergence in the number of degrees of freedom until convergence plateaus at around the level of machine precision.

**3.3. Higher-Order Integral equations.** The approach outlined in the previous few examples extends readily to higher-order integral equations of half-integer order. The general form of the problem we consider is

$$\mathcal{L}u(x) = e(x) + \sqrt{1+x}f(x) \quad (3.24)$$

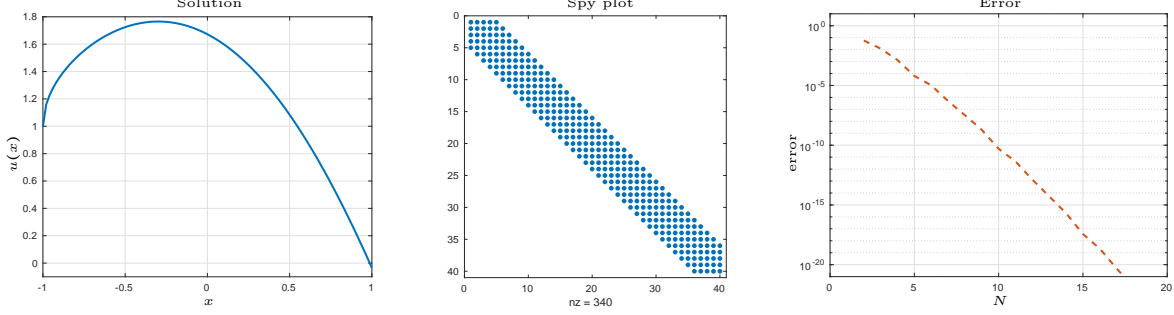


FIG. 3.4. (a) Approximate solution to (3.28) when  $N = 20$ . (b) MATLAB spy plot of (3.29) when  $N = 20$ . (c) 2-norm difference between the coefficients of the approximated solution when truncating at sizes  $N$  and  $\lceil 1.1N \rceil$ .

where

$$\mathcal{L}u(x) = \alpha^{[0]}(x)u(x) + \sum_{k=1}^{2m} \alpha^{[k]}(x) {}_{-1}\mathcal{Q}_x^{k/2}[\beta^{[k]}u](x), \quad (3.25)$$

$$\alpha^{[k]}(x) = p^{[k]}(x) + \sqrt{1+x}q^{[k]}(x), \quad \beta^{[k]}(x) = r^{[k]}(x) + \sqrt{1+x}s^{[k]}(x), \quad k = 0, 1, \dots, 2m, \quad (3.26)$$

and all the functions  $e(x), f(x), p^{[k]}(x), q^{[k]}(x), r^{[k]}(x), s^{[k]}(x), k = 0, 1, \dots, 2m$  are assumed analytic in some neighbourhood of  $[-1, 1]$ . If we continue to take (3.2) as our ansatz, then we arrive at the infinite dimensional linear system

$$\left( \Pi_0[p^{[0]}, q^{[0]}] + \sum_{k=1}^{2m} \Pi_0[p^{[k]}, q^{[k]}]Q^{k/2}\Pi_0[r^{[k]}, s^{[k]}] \right) \begin{pmatrix} \underline{a} \\ \underline{b} \end{pmatrix} = \begin{pmatrix} \underline{e} \\ \underline{f} \end{pmatrix}, \quad (3.27)$$

where  $\underline{e}$  and  $\underline{f}$  are as in (3.6).

As before, the precise form of this operator will depend on both  $m$  and the number of Chebyshev or Legendre coefficients required to represent the functions  $p^{[k]}, q^{[k]}, r^{[k]}$ , and  $s^{[k]}$ . However, if the  $q^{[k]}$  and  $s^{[k]}$  are all identically zero, then (after re-ordering) the operator will remain banded independently of  $N$ . Otherwise it will be lower-bounded, as in Example 3.

**Example 4:** For simplicity, we choose a constant coefficient problem so that the banded structure of the resulting operator is readily observed. In particular, we solve

$$u(x) - {}_{-1}\mathcal{Q}_x^{1/2}u(x) + {}_{-1}\mathcal{Q}_x^1u(x) - {}_{-1}\mathcal{Q}_x^{3/2}u(x) + {}_{-1}\mathcal{Q}_x^2u(x) = 1, \quad (3.28)$$

which may be expressed as

$$(I - Q^{1/2} + Q^1 - Q^{3/2} + Q^2) \begin{pmatrix} \underline{a} \\ \underline{b} \end{pmatrix} = \begin{pmatrix} 1 \\ 0 \end{pmatrix}. \quad (3.29)$$

As in the previous examples, we truncate this operator at a given size  $N$  and solve the resulting finite dimensional problem. The results are shown in Figure 3.4 with the first and second panels showing the approximated solution and spy plot of (3.29) when  $N = 20$ , respectively. The third panel shows the estimated accuracy of the solution. As in the Example 3 we do not know the true solution, so we estimate the error by the 2-norm difference between the coefficients of the approximated solution when truncating at sizes  $N$  and  $\lceil 1.1N \rceil$ . We again observe geometric convergence, and as in Example 1, the error continues to decrease even below the level of machine precision for this constant coefficient problem.

**4. FDEs: Riemann–Liouville definition.** Our approach here for FDEs of RL-type will be similar to the FIEs above. The main difference will stem from the fact that the operators  $D^m$  and  $D^{m+1/2}$  defined in Section 2.6 no longer map to the same direct sum spaces and we must make use of the block-banded conversion operators  $E_m$  and  $E_{m+1/2}$  (analogous to how the conversion operators  $\mathcal{S}_\lambda$  are used in [27]).

**4.1. Differential equation of order 1/2.** Consider the FDE

$$u(x) + {}_{-1}^{RL}D_x^{1/2}u(x) = e(x) + \frac{1}{\sqrt{1+x}}f(x), \quad x \in [-1, 1], \quad u(-1) < \infty, \quad (4.1)$$

(sometimes called a “fractional relaxation equation”) and make the same ansatz as before that

$$u(x) = \sum_{n=0}^{\infty} a_n P_n(x) + \sqrt{1+x} \sum_{n=0}^{\infty} b_n U_n(x) = [\mathbf{P}(x), \mathbf{U}_{1/2}(x)] \begin{pmatrix} \underline{a} \\ \underline{b} \end{pmatrix}. \quad (4.2)$$

From Section 2.6 we have that

$${}_{-1}^{RL}D_x^{1/2}u(x) = [\mathbf{C}^{(3/2)}(x), \mathbf{U}_{-1/2}(x)] D^{1/2} \begin{pmatrix} \underline{a} \\ \underline{b} \end{pmatrix}, \quad (4.3)$$

where  $D^{1/2}$  is defined in (2.39). As mentioned above, and unlike in the case of the integral equations, the range of  ${}_{-1}^{RL}D_x^{1/2}u(x)$  is not the same as that of  $u(x)$ . However, we can find a banded transform using  $E_{1/2}$  so that

$$u = [\mathbf{C}^{(3/2)}(x), \mathbf{U}_{-1/2}(x)] E_{1/2} \begin{pmatrix} \underline{a} \\ \underline{b} \end{pmatrix}. \quad (4.4)$$

This time letting

$$e(x) + \frac{1}{\sqrt{1+x}}f(x) = [\mathbf{C}^{(3/2)}(x), \mathbf{U}_{-1/2}(x)] \begin{pmatrix} \underline{e} \\ \underline{f} \end{pmatrix} \quad (4.5)$$

and equating coefficients leads to the linear system of equations

$$\begin{pmatrix} E_{1/2} + D^{1/2} \end{pmatrix} \begin{pmatrix} \underline{a} \\ \underline{b} \end{pmatrix} = \begin{pmatrix} S_{\mathbf{P}} & D_{\mathbf{U}_{1/2}}^{1/2} \\ D_{\mathbf{P}}^{1/2} & R_{\mathbf{U}} \end{pmatrix} \begin{pmatrix} \underline{a} \\ \underline{b} \end{pmatrix} = \begin{pmatrix} \underline{e} \\ \underline{f} \end{pmatrix}. \quad (4.6)$$

Again, each block of the operators in (4.6) are banded, and by interleaving the coefficients so that  $(\underline{a}^\top, \underline{b}^\top) \mapsto (a_0, b_0, a_1, b_1, \dots)^\top$  we can convert the above to a banded system.

**Remark:** One can show that the null space of the operator on the left-hand side of (4.1) acting on functions in  $L_1$  is

$$v(x) = \frac{E_{1/2,1/2}(-\sqrt{1+x})}{\sqrt{1+x}}, \quad (4.7)$$

(where  $E_{1/2,1/2}$  is the Mittag-Leffler function [13, 10.46.3]) [7, p. 13], which is unbounded at  $x = -1$ . Since our trial space (4.2) contains only bounded functions on  $[-1, 1]$ , we need not enforce a boundary condition explicitly in this case. We discuss boundary constraints in more detail momentarily. To allow solutions which are unbounded at the left end of the domain then one possibility is to use instead the ansatz  $u(x) = \mathbf{P}(x)\underline{a} + \mathbf{T}_{-1/2}(x)\underline{b}$ , where  $\mathbf{T}(x)$  is the quasimatrix whose columns are formed of Chebyshev polynomials of the first kind,  $T_n(x)$ ,  $n = 0, 1, \dots$ . One can derive similar banded operators to all those introduced in Section 2, but we omit the details (which are complicated by the fact that  $T_n(x)$  is not an ultraspherical polynomial and therefore many of the formulae in Section 2 differ subtly).

**Example 5:** We consider a modification of the second-kind Abel integral equation in Example 1, namely

$$u(x) + {}_{-1}D_x^{1/2}u(x) = \frac{1}{\sqrt{\pi}\sqrt{1+x}}, \quad u(-1) < \infty, \quad (4.8)$$

with solution

$$u(x) = e^{1+x} \operatorname{erfc}(\sqrt{1+x}). \quad (4.9)$$

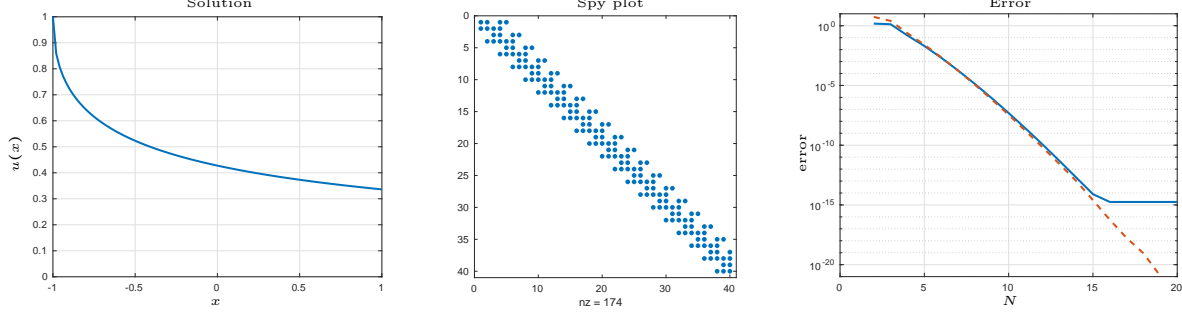


FIG. 4.1. (a) Approximate solution to (4.8) when  $N = 20$ . (b) MATLAB spy plot of (4.6) when  $N = 20$ . (c) Two measures of the error in the approximation as  $N$  varies. Solid line: Infinity norm error of solution approximated on a 100-point equally spaced grid. Dashed line: 2-norm difference between the coefficients of the approximated solution when truncating at sizes  $N$  and  $\lceil 1.1N \rceil$ .

To solve using our scheme we choose an  $N$  and form the system (4.6) with  $\underline{e} = \underline{0}$  and  $\underline{f} = [1/\sqrt{\pi}, 0, 0, \dots]^\top$ . Results are shown in Figure 4.1. As usual, the first two panels show a plot of the solution and a spy plot of the discretised operator when  $N = 20$ . The spy plot verifies that the matrix is banded (here with bandwidth four) and hence that the system (4.6) can be solved in linear time with MATLAB's `\`. The final panel shows both the infinity norm error (approximated on a 100-point equally spaced grid) of computed solution compared to the exact solution (4.9) (solid line) and the 2-norm difference between the coefficients of the approximated solution when truncating at sizes  $N$  and  $\lceil 1.1N \rceil$  (dashed line). Again we observe geometric convergence.

#### 4.2. Differential equation of order 1 and 1/2. Here we consider

$$u(x) + {}_{-1}^{RL}D_x^{1/2}u(x) + u'(x) = e(x) + \frac{1}{\sqrt{1+x}}f(x), \quad x \in [-1, 1], \quad (4.10)$$

along with a suitable initial or boundary condition, or some other functional constraint (see below). Now

$$u'(x) = \left[ \mathbf{C}^{(3/2)}(x), \mathbf{C}_{-1/2}^{(2)}(x) \right] D \left( \begin{array}{c} a \\ b \end{array} \right), \quad (4.11)$$

where  $D$  is defined in (2.39). We must also modify the spaces of both  $u(x)$  and  ${}_{-1}^{RL}D_x^{1/2}u(x)$  accordingly and so arrive at

$$\left( E_1 E_{1/2} + E_1 D^{1/2} + D \right) \left( \begin{array}{c} a \\ b \end{array} \right) = \left( \begin{array}{c} \underline{e} \\ \underline{f} \end{array} \right), \quad (4.12)$$

where

$$e(x) = \sum_{n=0}^{\infty} e_n C_n^{(3/2)}(x), \quad f(x) = \sum_{n=0}^{\infty} f_n C_n^{(2)}(x). \quad (4.13)$$

Again, by interleaving the coefficients, we can make the above operator banded.

**4.2.1. Boundary conditions.** In this case, the kernel of the operator in (4.10) is smooth and we must enforce a boundary condition to ensure that the linear system (4.12) is invertible. The topic of boundary conditions in FDEs is complicated, and it is beyond the scope of this paper to give a full treatment here. Here we simply show how certain boundary conditions/side constraints can be applied to the linear systems such as (4.12) and leave it to the reader to determine how many and what form of constraints are applicable to their FDE.

For example, consider the functional constraint  $\mathcal{B}^x u := u(x) = c$ . Given scalar  $x \in [-1, 1]$  we can construct this functional acting on a basis in  $\mathbf{C}_\gamma^{(\lambda)}$  as a row vector by defining  $B_{\lambda, \gamma}^x : \mathbf{C}_\gamma^{(\lambda)} \rightarrow \mathbb{C}$  as  $B_{\lambda, \gamma}^x := \mathbf{C}_\gamma^{(\lambda)}(x)$ . In

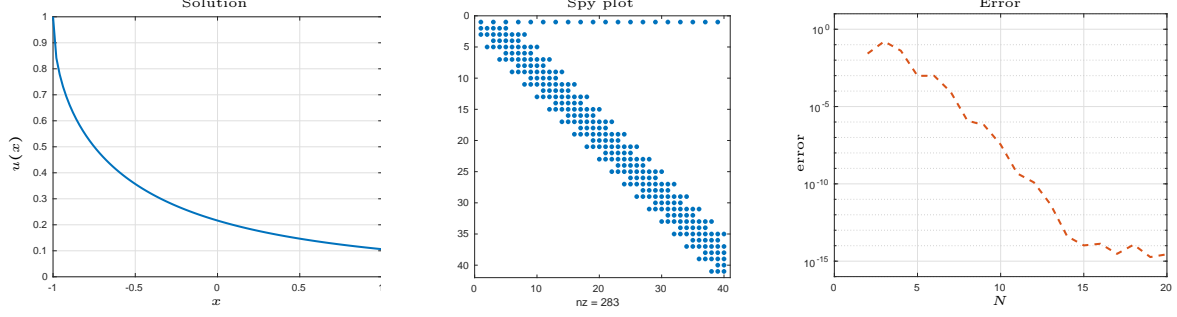


FIG. 4.2. (a) Approximate solution to (4.16) when  $N = 20$ . (b) MATLAB spy plot of (4.15) when  $N = 20$ . (c) Two measures of the error in the approximation as  $N$  varies. Solid line: Infinity norm error of solution approximated on a 100-point equally spaced grid. Dashed line: 2-norm difference between the coefficients of the approximated solution when truncating at sizes  $N$  and  $[1.1N]$ .

particular,  $x = -1$  corresponds to a boundary/initial condition on the left and  $x = +1$  to a boundary condition on the right, and some useful cases are

$$B_{\mathbf{P}}^{-1} = [1, -1, 1, -1, \dots], \quad B_{\mathbf{U}_{1/2}}^{-1} = [0, 0, \dots], \quad B_{\mathbf{P}}^{+1} = [1, 1, \dots], \quad \text{and} \quad B_{\mathbf{U}_{1/2}}^{+1} = \sqrt{2}[1, 2, 3, 4, \dots]. \quad (4.14)$$

Combining such operators to act on our direct sum expansion of the solution  $u(x)$ , we have, for example,  $B^{-1} : \mathbf{P} \oplus \mathbf{U}_{1/2} \rightarrow \mathbb{C}$  given by  $B^{-1} = [B_{\mathbf{P}}^{-1}, B_{\mathbf{U}_{1/2}}^{-1}]$  and our system (4.12) augmented with the boundary condition  $u(-1) = c$  becomes

$$\begin{pmatrix} B^{-1} \\ E_1 E_{1/2} + E_1 D^{1/2} + D \end{pmatrix} \begin{pmatrix} \underline{a} \\ \underline{b} \end{pmatrix} = \begin{pmatrix} c \\ \underline{e} \\ \underline{f} \end{pmatrix}, \quad (4.15)$$

Upon the usual re-ordering of the coefficients, this becomes an *almost-banded* infinite matrix—that is, banded apart from a finite number of dense rows—and when truncated to a  $(2N+1) \times (2N+1)$  finite matrix is solvable in  $O(N)$  operations using either a Schur complement factorisation about the (1,1) entry, the Woodbury matrix identity, or by using the adaptive QR method described in [27]. See Section 6.2 for more details.

**Example 6:** Consider the case of (4.10) where the right-hand side is zero and  $u(-1) = 1$ :

$$u(x) + {}^{RL}_{-1}D_x^{1/2}u(x) + u'(x) = 0, \quad x \in [-1, 1], \quad (4.16)$$

which amounts to taking  $c = 1$  and  $\underline{e} = \underline{f} = \underline{0}$  in (4.15). The computed solution is depicted in the left panel of Figure 4.2. The middle panel verifies the almost banded nature of the operator (4.15), and the right panel demonstrates geometric convergence.

**4.3. Non-constant coefficients.** Non-constant coefficients can be dealt with in a similar way as described for fractional integral equations in Section 3.2. We omit the details.

**4.4. Higher order.** Similarly to the case of integral equations, the approach outlined above can be extended to higher-order derivatives. Consider the general  $m$ th half-integer order FDE:

$$\mathcal{L}u(x) = \alpha^{[0]}(x)u(x) + \sum_{k=1}^{2m} \alpha^{[k]}(x) {}_{-1}\mathcal{D}_x^{k/2}[\beta^{[k]}u](x), \quad (4.17)$$

where the nonconstant coefficients  $\alpha^{[k]}(x)$  and  $\beta^{[k]}(x)$  are analytic in some neighbourhood of  $[-1, 1]$ . If we continue to take as our ansatz solution the function

$$u(x) = [\mathbf{P}(x), \mathbf{U}_{1/2}(x)] \begin{pmatrix} \underline{a} \\ \underline{b} \end{pmatrix} \quad (4.18)$$



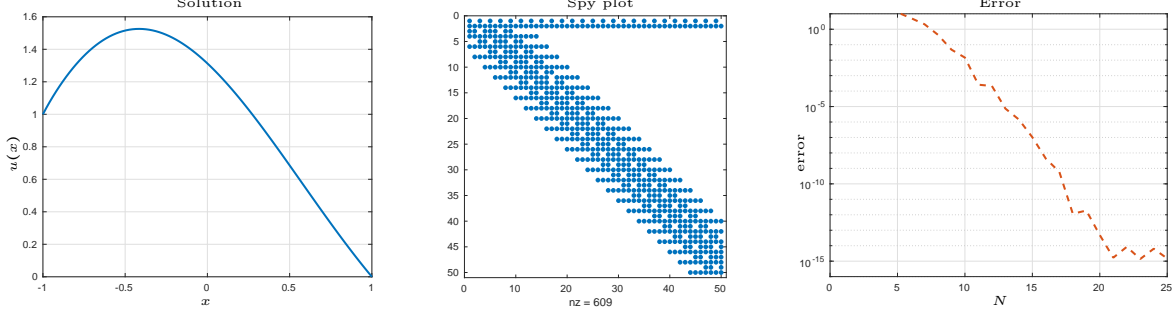


FIG. 4.3. (a) Approximate solution to the Bagley–Torvik equation (4.20) when  $N = 25$ . (b) MATLAB spy plot of (4.22) when  $N = 25$ . (c) 2-norm difference between the coefficients of the approximated solution when truncating at sizes  $N$  and  $[1.1N]$ .

then we have  $L : \mathbf{P} \oplus \mathbf{U}_{1/2} \rightarrow \mathbf{C}^{(m+1/2)} \oplus \mathbf{C}_{-m+1/2}^{(m+1)}$  given by

$$\left( \sum_{k=0}^{2m-1} (E_m E_{m-1/2} \dots E_{(k+1)/2}) \Pi_{k/2} [\alpha^{[k]}, \cdot] D^{k/2} \Pi[\beta^{[k]}, \cdot] \right) + \Pi_m [\alpha^{[2m]}, \cdot] D^m \Pi[\beta^{[2m]}, \cdot] \quad (4.19)$$

(where we have defined  $\beta^{[0]}(x) = 1$  for the sake of brevity).

**Example 7:** Consider the classical Bagley–Torvik equation [5, 6]

$$u''(x) + {}^{RL}_{-1}D_x^{1/2}u(x) + u(x) = 0, \quad x \in [-1, 1] \quad (4.20)$$

but here treated as a boundary value problem with

$$u(-1) = 1, \quad \text{and} \quad u(1) = 0. \quad (4.21)$$

Following the approach outlined above, we arrive at the infinite dimensional linear system

$$\begin{pmatrix} B^{-1} \\ B^{+1} \\ D^2 + E_2 E_{3/2} E_1 (D^{1/2} + E_{1/2}) \end{pmatrix} \begin{pmatrix} a \\ b \\ \underline{f} \end{pmatrix} = \begin{pmatrix} 0 \\ 1 \\ \underline{e} \end{pmatrix}, \quad (4.22)$$

which can be solved in the same manner as before. The solution is depicted in Figure 4.3.

**Remark:** If we instead consider the FDE:  $u''(x) + {}^{RL}_{-1}D_x^{3/2}u(x) + u(x) = 0$ , then we simply change the final block-row of the system (4.22) to  $D^2 + E_2(D^{3/2} + E_{3/2}E_1E_{1/2})$ . Similarly, we could incorporate a Neumann or fractional Neumann boundary condition at, say, the right boundary by changing the  $B^{+1}$  row to the appropriate functional row.

**5. FDEs: Caputo definition.** FDEs with the Caputo definition of the fractional derivative can be readily solved by combining our approach for FIEs described in Section 3 with an integral reformulation of the problem. In particular, setting  $v(x) = u^{([m])}(x)$  and therefore  $u(x) = Q^{[m]}v(x) + p(x)$ ,  $p(x) \in \mathbb{P}^{[m]-1}$ , it follows from the definition of the Caputo derivative that an  $m$ th-order FDE in  $u(x)$  becomes an  $m$ th-order FIE in  $v(x)$  with  $[m]$  additional boundary constraints to determine the coefficients of the polynomial  $p(x) = c_0 + c_1 P_1(x) + \dots + c_{[m]-1} P^{[m]-1}(x)$ . We proceed by example.

**Example 8:** Consider the Caputo fractional relaxation equation

$$u(x) + {}^C_{-1}\mathcal{D}_x^{1/2}u(x) = 0, \quad u(-1) = 1, \quad (5.1)$$

which also has the solution

$$u(x) = e^{1+x} \operatorname{erfc}(\sqrt{1+x}). \quad (5.2)$$

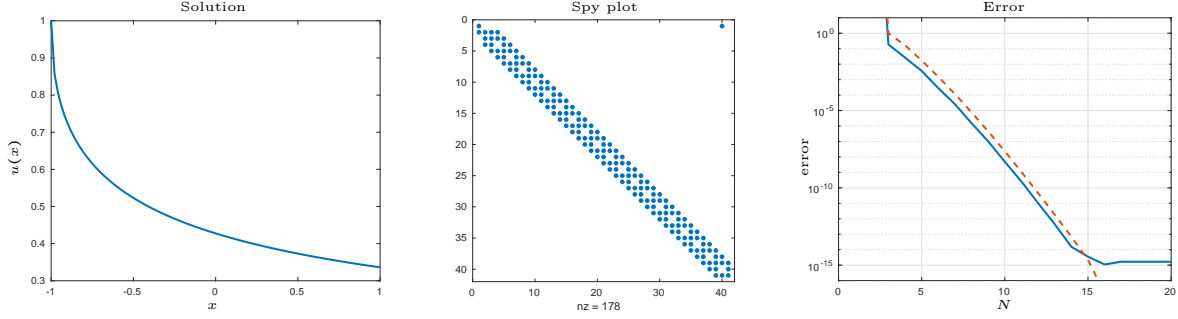


FIG. 5.1. (a) Approximate solution to the FDE (5.1) when  $N = 20$ . (b) MATLAB spy plot of (5.5) when  $N = 20$ . (c) Two measures of the error in the approximation as  $N$  varies. Solid line: Infinity norm error of solution approximated on a 100-point equally spaced grid. Dashed line: 2-norm difference between the coefficients of the approximated solution when truncating at sizes  $N$  and  $[1.1N]$ .

Letting  $v = u'$  we have  $u = \mathcal{Q}v + c_0$  and (5.1) becomes

$$\mathcal{Q}v(x) + {}_{-1}\mathcal{Q}_x^{1/2}v(x) + c_0 = 0, \quad (5.3)$$

$$\mathcal{Q}v(-1) + c_0 = 1. \quad (5.4)$$

In operator form, we may write this as the infinite dimensional system

$$\begin{pmatrix} 1 & B^{-1}Q \\ \begin{bmatrix} \underline{e}_1 \\ \underline{0} \end{bmatrix} & Q + Q^{1/2} \end{pmatrix} \begin{pmatrix} c_0 \\ \begin{bmatrix} \hat{a} \\ \hat{b} \end{bmatrix} \end{pmatrix} = \begin{pmatrix} 1 \\ \underline{0} \end{pmatrix}, \quad (5.5)$$

where  $v(x) = \sum_{n=0}^{\infty} \hat{a}_n P_n(x) + \sqrt{1+x} \hat{b}_n U_n(x)$  and  $B^{-1} = [B_{\mathbf{P}}^{-1}, B_{\mathbf{U}_{1/2}}^{-1}]$ . After truncating and solving this system for the approximate coefficients of  $v$ , we can recover those of  $u$  via

$$\begin{pmatrix} \underline{a} \\ \underline{b} \end{pmatrix} = Q \begin{pmatrix} \hat{a} \\ \hat{b} \end{pmatrix} + \begin{pmatrix} c_0 \\ \underline{0} \end{pmatrix}. \quad (5.6)$$

Figure 5.1 shows the results.

**Example 9:** Consider the Bagley–Torvik equation from Example 7, but now using the Caputo definition of the half-derivative:

$$u''(x) + {}_C D_x^{1/2} u(x) + u(x) = 0, \quad x \in [-1, 1], \quad (5.7)$$

$$u(-1) = 1, \quad u(1) = 0. \quad (5.8)$$

This time letting  $v = u''$  we have  $u = \mathcal{Q}^2 v + c_0 P_0(x) + c_1 P_1(x)$  and

$$v(x) + {}_{-1}\mathcal{Q}_x^{3/2} v(x) + c_1 \mathcal{Q}_x^{1/2} P_1'(x) + \mathcal{Q}^2 v(x) + c_0 P_0(x) + c_1 P_1(x) = 0, \quad (5.9)$$

$$\mathcal{Q}^2 v(-1) + c_0 + c_1 P_1(-1) = 1, \quad (5.10)$$

$$\mathcal{Q}^2 v(1) + c_0 + c_1 P_1(1) = 0. \quad (5.11)$$

We may write this as

$$\begin{pmatrix} 1 & -1 & B^{-1}Q^2 \\ 1 & 1 & B^{+1}Q^2 \\ \begin{bmatrix} \underline{e}_1 \\ \underline{0} \end{bmatrix} & Q^{1/2} \begin{bmatrix} S_{1/2}^{-1} D_{1/2} \underline{e}_1 \\ \underline{0} \end{bmatrix} + \begin{bmatrix} \underline{e}_1 \\ \underline{0} \end{bmatrix} & Q^2 + Q^{3/2} + I \end{pmatrix} \begin{pmatrix} c_0 \\ c_1 \\ \begin{bmatrix} \hat{a} \\ \hat{b} \end{bmatrix} \end{pmatrix} = \begin{pmatrix} 1 \\ 0 \\ \begin{bmatrix} \underline{0} \\ \underline{0} \end{bmatrix} \end{pmatrix}, \quad (5.12)$$

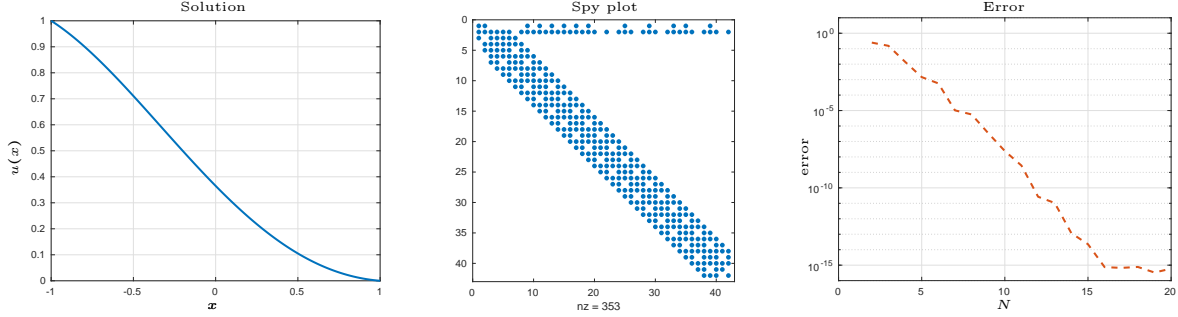


FIG. 5.2. (a) Approximate solution to (5.7) when  $N = 20$ . (b) MATLAB spy plot of (5.12) when  $N = 20$ . (c) Two measures of the error in the approximation as  $N$  varies. Solid line: Infinity norm error of solution approximated on a 100-point equally spaced grid. Dashed line: 2-norm difference between the coefficients of the approximated solution when truncating at sizes  $N$  and  $\lceil 1.1N \rceil$ .

where  $v(x) = \sum_{n=0}^{\infty} \hat{a}_n P_n(x) + \sqrt{1+x} \hat{b}_n U_n(x)$  and we have used the fact that  $P_1(\pm 1) = \pm 1$ . Once we have solved this system for the approximate coefficients of  $v$ , we can recover those of  $u$  via

$$\begin{pmatrix} \frac{a}{b} \end{pmatrix} = Q \begin{pmatrix} \frac{\hat{a}}{\hat{b}} \end{pmatrix} + \begin{pmatrix} c_0 \\ c_1 \\ \underline{0} \end{pmatrix}, \quad (5.13)$$

where here  $\underline{0}$  is a vector of zeros of length  $2N - 2$ . Figure 5.2 shows the results. Compare with Riemann–Liouville version in Example 7.

**6. Computational issues.** In this section we outline some practical considerations required to perform computations.

**6.1. Representing the right-hand side.** An essential part of this approach is representing the right-hand side in the direct sum basis  $\mathbf{P} \oplus \mathbf{U}_{1/2}$  and its higher-order cousins involving higher order ultraspherical polynomials. A substantial issue is that given a general right-hand side  $r(x)$  the decomposition as, for example,

$$r(x) = \sum_{n=0}^{\infty} e_n P_n(x) + \sqrt{1+x} \sum_{n=0}^{\infty} f_n U_n(x). \quad (6.1)$$

is not unique:  $P_n(x)$  and  $\sqrt{1+x}U_n(x)$  form a *frame* [9]. In the context of this numerical approach, uniqueness is not critical as any expansion of this form is suitable provided we can approximate  $f$  well by taking finite number of terms.

We will assume we are given  $e(x)$  and  $f(x)$  that can be evaluated pointwise<sup>6</sup> so that

$$r(x) = e(x) + \sqrt{1+x}f(x). \quad (6.2)$$

In this case, we can calculate the number of Chebyshev coefficients of  $e$  and/or  $f$  to within a required tolerance using an adaptive algorithm [4, 14]. The algorithm is based on the discrete cosine transform (DCT) and hence takes  $\mathcal{O}(d \log d)$  operations to compute  $d$  coefficients. Calculating coefficients in a basis  $\mathbf{C}^{(\lambda)}$ ,  $\lambda \in \mathbb{N}^+$  proceeds in  $\mathcal{O}(\lambda d)$  operations by applying the conversion operators (2.9). Calculating  $d$  Legendre coefficients from  $d$  Chebyshev coefficients can be accomplished in  $\mathcal{O}(d \log^2 d)$  operations using recently developed fast Chebyshev–Legendre transforms [17, 37], and from these coefficients in a basis  $\mathbf{C}^{(\lambda+1/2)}$ ,  $\lambda \in \mathbb{N}^+$  can again be calculated in  $\mathcal{O}(\lambda d)$  operations by the conversion operators (2.9). The coefficients in non-constant coefficient problems can be computed in an analogous manner.

<sup>6</sup>The case where we may only sample  $r(x)$  is beyond the scope of this paper, though solving a least squares system with more points than coefficients can perform well in practice. Another situation that arises in practical settings is where  $r(x)$  is specified by a formula such as  $\exp(x)\sqrt{1+x} + \cos x + \exp((1+x)/2)\operatorname{erfc}(\sqrt{1+x})$ . The approach taken by ApproxFun is to overload each operation to automatically determine an appropriate decomposition.

**Remark:** In typical applications  $d$  (the number of coefficients required to represent the right-hand side or non-constant terms) is much smaller than  $N$  (the discretisation size of the system) and the claim that the proposed method is linear in the degrees of freedom is justified. The exception is when the linear problem arises from the linearisation of a nonlinear problem. In this case the number of polynomial terms required to approximate the non-constant coefficients will be the same as the for the solution (i.e.,  $d \approx N$ ). The linear systems resulting from discretisation are then dense and require  $\mathcal{O}(N^3)$  operations to solve via Gaussian elimination. A spectrally accurate algorithm with linear complexity is still an open problem even in the case of ODEs.

**6.2. Solving the linear systems.** We have described an approach to reduce fractional differential and integral equations to banded or almost-banded infinite-dimensional linear systems. A natural approach to approximating the solutions to the resulting equations is the *finite section method*: truncate the infinite-dimensional systems to  $2N \times 2N$  finite-dimensional linear systems. This is an effective and easy to implement approach that achieves  $\mathcal{O}(N)$  complexity using standard LAPack routines in the banded case, or using the Woodbury formula in the almost-banded case.

Alternatively, one can solve using the adaptive QR method [27], which can be thought of as performing linear algebra directly on the infinite-dimensional linear system [28]. In this case, the number of coefficients needed to represent the solution within a specified tolerance of the error in residual are determined adaptively while preserving the linear complexity. A benefit of this approach, in addition to the adaptivity, is that it is not prone to discretization introducing ill-posed equations. Left and right half-integral and half-derivative operators are implemented in the ApproxFun.jl package [26] for Julia which uses the adaptive QR method.

**7. Conclusion.** By writing the solution in an appropriately constructed basis (in particular a direct sum of Legendre,  $P_n(x)$ , and weighted Chebyshev polynomials of the first kind,  $\sqrt{1+x}U_n(x)$ ) we have successfully solved a broad class of half-integer order fractional integral and differential equations with spectral accuracy in linear complexity. The main objective of this paper is to introduce the algorithm and demonstrate its applicability, and several examples of both constant and non-constant coefficient linear problems were presented. Some analysis of the half-integral equation described in Section 3.1 can be found in Section B.1.

There are several opportunities for future extensions. Nonlinear problems (through linearisation and Newton’s method), time-dependent problems (through method of lines), and partial fractional differential equations (FDPEs) on rectangular domains (using ideas related to [36]) should be relatively straightforward, and we hope to solve problems of this type in a future publication. While we have focused on half-order operators, it is possible that other rational powers ( $1/3$ ,  $1/4$ , etc.) may be tackled using a similar technique: represent the solution as a direct sum of a finite number (3, 4, etc.) of weighted Jacobi spaces. Furthermore, an open problem is adapting the approach to problems involving the two-sided fractional derivative, used to define the fractional Laplacian. The known formula for the fractional (or even half-) integral of Jacobi polynomials does not allow for weighting at both the left and right end of the domain simultaneously, which would be required to capture the singular behaviour of two-sided derivatives.

We close with one last example which demonstrates both the high accuracy and linear complexity of the approach described in this paper when applied to a more challenging problem than those shown in the previous few sections. In particular, let’s consider fractional Airy equations of the form

$$\varepsilon i^{3/2} {}_{-1}^{RL}D_x^{3/2}u(x) - xu(x) = 0, \quad x \in [-1, 1], \quad (7.1)$$

with  $\varepsilon > 0$  and boundary conditions  $u(-1) = 0$  and  $u(1) = 1$ . Although complex-valued, this non-constant coefficient FDE is of the form described in Section 4 and we may solve accordingly using the algorithm described. The first and second panels of Figure 7.1 show the real and imaginary parts of the solution for  $\varepsilon = 10^{-4}$ , and we see behaviour qualitatively similar to that of the well-known classical Airy equation. Experimentally we find that an accuracy of  $10^{-10}$  requires around 750 degrees of freedom (i.e.,  $N \approx 375$ ), and forming and solving the almost-banded linear system representing the fractional differential operator and boundary conditions takes around 0.1 seconds on a 2014 Desktop PC using a MATLAB implementation [16]. The third panel shows the computational times to form and solve the systems the number degrees of freedom is increased. Using the Woodbury formula to solve the almost-banded linear system, we see that linear

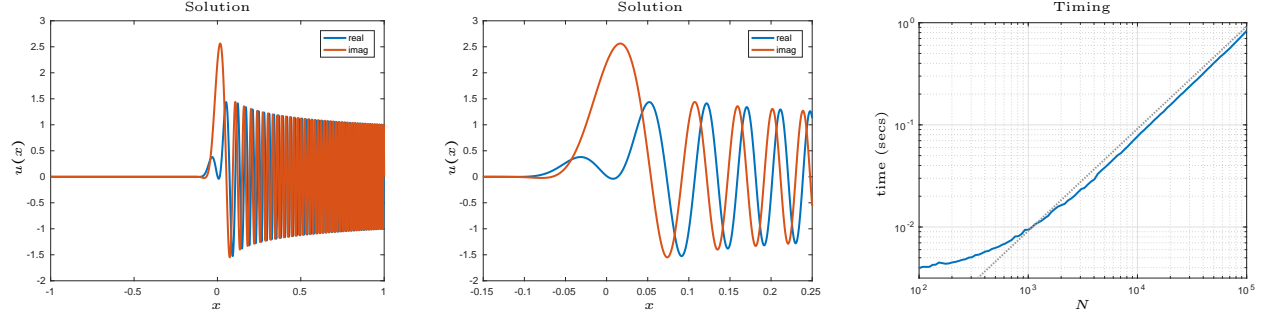


FIG. 7.1. (a) Approximate solution to the fractional Airy equation (7.1) with  $\varepsilon = 10^{-4}$ . (b) Close-up of the solution near the origin. (c) Timings for building and solving the linear system for increasing degrees of freedom.

complexity is obtained. Finally, we note that this Riemman–Louisville FDE can be readily solved using ApproxFun [26] with just a few commands:

```
using ApproxFun
S = Legendre() ⊕ JacobiWeight(0.5, 0, Ultraspherical(1))
T = Ultraspherical(2.5) ⊕ JacobiWeight(-1.5, 0, Ultraspherical(2))
D15 = LeftDerivative(1.5) : S ↦ T
x = Fun()
u = [dirichlet() ; 0.0001*im^1.5*D15 - x] \ [0 ; 1 ; 0]
```

TABLE 7.1

ApproxFun code for solving the fractional Airy equation (7.1) with  $\varepsilon = 0.0001$ .

**Acknowledgements.** We thank Daniel Hauer (U. Sydney) for discussions related to convergence in higher order norms, Marcus Webb (U. Cambridge) for discussions on fractional differential equations, and Alex Townsend (Cornell) for some useful suggestions.

**Appendix A. Miscellaneous proofs.** The following results are required in the proofs of Corollaries 2.2 and 2.3 in Sections 2.4 and 2.5, respectively.

LEMMA A.1. For any  $n > 0$  and  $\lambda > 0$ , the ultraspherical polynomials  $C_n^{(\lambda)}(x)$  satisfy the relationship:

$$2\lambda(1+x)(C_n^{(\lambda+1)}(x) - C_{n-1}^{(\lambda+1)}(x)) = ((n+1)C_{n+1}^{(\lambda)}(x) + (n+2\lambda)C_n^{(\lambda)}(x)). \quad (\text{A.1})$$

*Proof.* Applying (2.11) to  $C_n^{(\lambda+1)}(x)$  and  $C_{n-1}^{(\lambda+1)}(x)$  gives, upon rearrangement,

$$(1+x)(C_n^{(\lambda+1)}(x) - C_{n-1}^{(\lambda+1)}(x)) = \frac{1}{2} \frac{n+1}{n+\lambda+1} (C_{n+1}^{(\lambda+1)}(x) - C_{n-1}^{(\lambda+1)}(x)) + \frac{1}{2} \frac{n+2\lambda}{n+\lambda} (C_n^{(\lambda+1)}(x) - C_{n-2}^{(\lambda+1)}(x)). \quad (\text{A.2})$$

Applying (2.8) to each of the bracketed terms on the right-hand side and cancelling common terms gives the required result.  $\square$

COROLLARY A.2. The Legendre polynomials,  $P_n(x)$ , and the Chebyshev polynomials,  $U_n(x)$ , satisfy

$$n(P_n(x) + P_{n-1}(x)) = (1+x)(C_{n-1}^{(3/2)}(x) - C_{n-2}^{(3/2)}(x)) \quad (\text{A.3})$$

and

$$U_n(x) + (n+1)U_{n-1}(x) = 2(1+x)(C_{n-1}^{(2)}(x) - C_{n-2}^{(2)}(x)). \quad (\text{A.4})$$

*Proof.* Take  $n \mapsto n-1$  with  $\lambda = \frac{1}{2}$  and  $\lambda = 1$  in (A.1), respectively.  $\square$

**Appendix B. Convergence and stability results.**

**B.1. Convergence.** Note that the decompositions of the right-hand side and solution of (3.1) in the forms (3.2) and (3.6) are not unique, so the well-posedness of (3.8) is not immediate. However, the Schur complement of the (1, 1) block of (3.8) yields

$$\begin{aligned} (Q_{\mathbf{P}} - \sigma^2 I)\underline{a} &= Q_{\mathbf{U}}^{1/2} \underline{f} - \sigma \underline{e}, \\ \sigma \underline{b} &= \underline{f} - Q_{\mathbf{P}}^{1/2} \underline{a}, \end{aligned} \quad (\text{B.1})$$

where  $Q_{\mathbf{P}} = Q_{\mathbf{U}}^{1/2} Q_{\mathbf{P}}^{1/2}$  is the indefinite integral operator acting on the Legendre basis (recall (2.23)). The fact that  $Q_{\mathbf{P}}$  is banded along with the decaying properties of its entries leads to a proof of convergence whenever the original equation (3.1) is solvable in  $L^2[-1, 1]$ .

DEFINITION B.1. Define the Banach space  $\ell_\lambda^2$  with norm

$$\|\underline{f}\|_{\ell_\lambda^2}^2 = \sum_{k=0}^{\infty} (k+1)^{2\lambda} f_k^2. \quad (\text{B.2})$$

LEMMA B.2. Let  $\Psi := \text{diag}\left(\sqrt{2}, \sqrt{\frac{2}{3}}, \sqrt{\frac{2}{5}}, \sqrt{\frac{2}{7}}, \dots\right)$ . If  $\sigma^2$  is an  $\ell^2$  eigenvalue of  $\tilde{Q}_{\mathbf{P}} := \Psi Q_{\mathbf{P}} \Psi^{-1}$ , then  $\sigma$  is an  $L^2[-1, 1]$  eigenvalue of  ${}_{-1}\mathcal{Q}_x^{1/2}$ .

*Proof.* Note that  $\|P_n\| = \sqrt{\frac{2}{2n+1}}$ , hence conjugating by  $\Psi$  recasts the operator to acting on expansions in the orthonormalized Legendre polynomials  $\tilde{P}_n(x) := P_n(x)\sqrt{\frac{2n+1}{2}}$ . The assumption on  $\sigma^2$  being an  $\ell^2$  eigenvalue enforces that any eigenvector  $\underline{a}$  of  $\tilde{Q}_{\mathbf{P}}$  corresponds to the normalized Legendre coefficients of a function  $a(x)$  in  $L^2[-1, 1]$ , with norm  $\|\underline{a}\|_{\ell^2}$ .

The entries of  $\tilde{Q}_{\mathbf{P}}$  decay like  $1/k$ , which implies that  $\tilde{Q}_{\mathbf{P}} : \ell_\lambda^2 \rightarrow \ell_{\lambda+1}^2$ . It follows immediately that the  $\underline{a} \in \ell_\lambda^2$  for all  $\lambda$ ; in particular,  $\underline{a} \in \ell^1$ . We can bound

$$\|\sqrt{1+x}U_k\|^2 = \int_{-1}^1 (1+x) \frac{\sin^2(k+1)\cos^{-1}x}{\sin^2 x} dx = \int_0^\pi (1+\cos\theta) \frac{\sin^2(k+1)\theta}{\sin\theta} d\theta \leq 2\pi(k+1) \quad (\text{B.3})$$

since Lagrange's trigonometric identities ensure that

$$\left| \frac{\sin(k+1)\theta}{\sin\theta} \right| \leq k+1. \quad (\text{B.4})$$

Thus the  $O(1/\sqrt{k})$  decay in  $Q_{\mathbf{P}}^{1/2}\Psi^{-1}$  cancels the  $O(\sqrt{k})$  growth from  $\|\sqrt{1+x}U_k\|$ , and we have

$$\left\| \left( \sqrt{1+x}U_0(x), \sqrt{1+x}U_1(x), \dots \right) Q_{\mathbf{P}}^{1/2}\Psi^{-1}\underline{a} \right\| \leq C\|\underline{a}\|_{\ell^1} < \infty. \quad (\text{B.5})$$

That is, the entries of  $\underline{b} = -Q_{\mathbf{P}}^{1/2}\Psi^{-1}\underline{a}$  correspond to the second-kind Chebyshev coefficients of a function  $b(x)$  such that  $\sqrt{1+x}b(x)$  is in  $L^2[-1, 1]$ . We therefore have an  $L^2[-1, 1]$  eigenvector  $a(x) + \sqrt{1+x}b(x)$ .  $\square$

LEMMA B.3. If  $\sigma I + {}_{-1}\mathcal{Q}_x^{1/2}$  is invertible in  $L^2[-1, 1]$  then  $\sigma^2 I + \tilde{Q}_{\mathbf{P}}$  is invertible in  $\ell_\lambda^2$  for all  $\lambda > 0$  and in  $\ell^1$ . If  $\underline{e}, \underline{f} \in \ell^1$ , and  $\underline{a} = (\sigma^2 I + \tilde{Q}_{\mathbf{P}})^{-1}(Q_{\mathbf{U}}^{1/2}\underline{f} - \sigma \underline{e})$ , then  $a(x) + \sqrt{1+x}b(x) = (\sigma I + {}_{-1}\mathcal{Q}_x^{1/2})^{-1}(e(x) + \sqrt{1+x}f(x))$  for  $e(x) = \mathbf{P}(x)\underline{e}$ ,  $f(x) = \mathbf{U}_{1/2}(x)\underline{f}$ ,  $a(x) = \mathbf{P}(x)\underline{a}$  and  $b(x) = \sigma^{-1}(f(x) - \mathbf{U}_{1/2}(x)Q_{\mathbf{P}}^{1/2}\underline{a})$ .

*Proof.* The decay in the entries of  $\tilde{Q}_{\mathbf{P}}$  and bandedness imply that  $\|P_N \tilde{Q}_{\mathbf{P}} - \tilde{Q}_{\mathbf{P}}\|_{\ell_\lambda^2} \rightarrow 0$ :  $\tilde{Q}_{\mathbf{P}}$  is compact in  $\ell_\lambda^2$  (and by a similar argument, in  $\ell^1$ ). Compactness guarantees that the operator only has discrete eigenvalues. However, the previous lemma ensures that if  $\sigma I + {}_{-1}\mathcal{Q}_x^{1/2}$  is invertible in  $L^2[-1, 1]$ , then  $\sigma^2$  is not an  $\ell^2$  eigenvalue of  $\tilde{Q}_{\mathbf{P}}$ , and hence  $\sigma^2 I + \tilde{Q}_{\mathbf{P}}$  is invertible in  $\ell^2$ . But any  $\ell^2$  eigenvector is an eigenvector in  $\ell_\lambda^2$  for all  $\lambda$  (and in  $\ell^1$ ) as  $\tilde{Q}_{\mathbf{P}}$  induces additional decay, and trivially, any  $\ell_\lambda^2$  eigenvector is automatically an  $\ell^2$  eigenvector. Thus we know that  $\sigma^2$  is also not an  $\ell_\lambda^2$  (or  $\ell^1$ ) eigenvalue, and the operator is invertible.

Therefore, if  $\underline{e}, \underline{f} \in \ell^1$  then  $\underline{a} \in \ell^1$ , hence (by the logic of the previous lemma)  $a(x) + \sqrt{1+x}b(x) \in L^2[-1, 1]$ . We have thus constructed the unique  $L^2[-1, 1]$  solution of  $(\sigma I + {}_{-1}\mathcal{Q}_x^{1/2})u(x) = e(x) + \sqrt{1+x}f(x)$   $\square$

We now consider the finite section approximation of (3.8), i.e., we define the projection operator  $P_N : \ell^2 \rightarrow \mathbb{R}^N$  and consider the  $2N \times 2N$  finite section approximation

$$\begin{pmatrix} \sigma I_N & P_N Q_{\mathbf{U}}^{1/2} P_N^\top \\ P_N Q_{\mathbf{P}}^{1/2} P_N^\top & \sigma I_N \end{pmatrix} \begin{pmatrix} \underline{a}_N \\ \underline{b}_N \end{pmatrix} = \begin{pmatrix} P_N \underline{e} \\ P_N \underline{f} \end{pmatrix}. \quad (\text{B.6})$$

This leads to an approximation

$$\begin{aligned} a(x) &\approx a_N(x) = \mathbf{P}(x) \underline{a}_N \\ b(x) &\approx b_N(x) = \sigma^{-1} \mathbf{U}(x) (P_N \underline{f} - Q_{\mathbf{P}}^{1/2} \underline{a}_N) \\ u(x) &\approx u_N(x) = a_N(x) + \sqrt{1+x} b_N(x). \end{aligned} \quad (\text{B.7})$$

**THEOREM B.4.** *If  $\sigma I +_{-1} Q_x^{1/2}$  is invertible in  $L^2[-1,1]$  and  $\underline{e}, \underline{f}$  are in  $\ell^1$ , then the finite section approximation to (B.1)  $u_N$  converges to the true solution of (3.1) in  $L^2[-1,1]$ .*

*Proof.* Note that, because  $Q_{\mathbf{P}}^{1/2}$  is upper triangular and  $Q_{\mathbf{U}}^{1/2}$  is lower triangular, we have

$$P_N Q_{\mathbf{U}}^{1/2} P_N^\top P_N Q_{\mathbf{P}}^{1/2} P_N^\top = P_N Q_{\mathbf{U}}^{1/2} Q_{\mathbf{P}}^{1/2} P_N^\top = P_N Q_{\mathbf{P}} P_N^\top. \quad (\text{B.8})$$

It follows that  $\underline{a}_N$  is also a solution to the  $n \times n$  finite section of (B.1):

$$P_N (Q_{\mathbf{P}} - \sigma^2 I) P_N^\top \underline{a}_N = P_N (Q_{\mathbf{U}}^{1/2} \underline{f} - \sigma \underline{e}). \quad (\text{B.9})$$

If the condition of this theorem holds, then by the previous lemma,  $\sigma^2$  is not an eigenvalue of  $\tilde{Q}_{\mathbf{P}}$ .  $\tilde{Q}_{\mathbf{P}}$  is a compact operator on  $\ell^1$ , therefore the finite-section approximation  $\underline{a}_N$  converges to  $\underline{a}$  in an  $\ell^1$  sense (this follows from a Neumann series argument, see e.g., [27, Theorem 4.5]). This implies convergence of  $a_N(x)$  to  $a(x)$  in  $L^2[-1,1]$  and convergence of  $b_N(x)$  to  $b(x)$  in  $L^2[-1,1]$ , thence  $u_N(x)$  converges to  $u(x)$  in  $L^2[-1,1]$ .  $\square$

**COROLLARY B.5.** *Provided that  $\underline{e}, \underline{f} \in \ell_\lambda^2$ , the finite section approximation converges in  $\ell_\lambda^2$ . If this condition holds for all  $\lambda$ , then  $u_N$  converges in  $L^2[-1,1]$  at a spectrally fast rate. Similarly, if  $\underline{e}, \underline{f}$  decay exponentially, then  $u_N$  converges in  $L^2[-1,1]$  exponentially fast.*

*Proof.* The first statement follows from the operator being a compact perturbation of the identity in all  $\ell_\lambda^2$  spaces, hence the same argument as Theorem B.4 applies. The second statement follows from relating convergence in  $\ell_\lambda^2$  to fast convergence in  $\ell^1$ . The exponentially fast convergence follows similarly by adapting the results to the norm  $\sqrt{\sum_{k=0}^\infty |R^k f_k|^2}$ .  $\square$

**B.2. Stability.** Unfortunately, solvability of the resulting equation is not the only issue: we must also consider conditioning. Now,  $v(x) = e^{x/\sigma^2}$  is the solution to  $Qu(x) - \sigma^2 u(x) = e^{-1/\sigma^2}$ , hence, for  $\sigma \ll 1$ ,  $v(x)$  is approximately in the kernel of  $Qu(x) - \sigma^2 I$ . Therefore, we should expect the solution of the above system, and hence the system (3.8) to be ill-conditioned when  $\sigma \ll 1$ . Indeed, the pseudo-spectral plot of the two (truncated) linear systems in Figure B.2 confirms this.

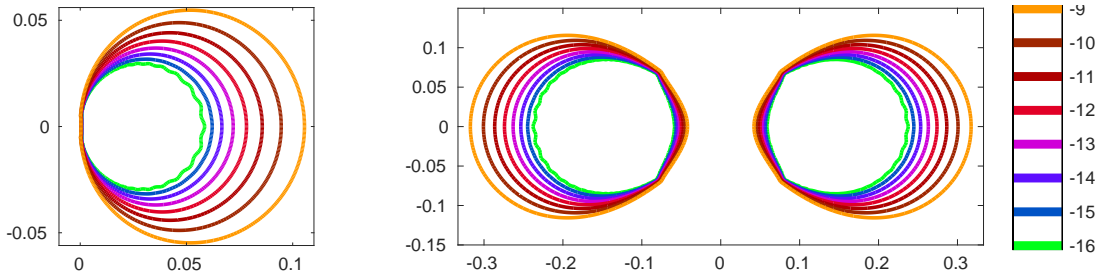


FIG. B.1. Left: Pseudospectra (computing using EigTool [39]) of the operator  $Q_{1/2}$  truncated to a  $200 \times 200$  matrix. Right: The same for (3.8) with  $\sigma = 0$ .

Decreasing  $\sigma$  in this way is equivalent to a change of variables from  $[-1, 1]$  to a longer ‘time’ domain (if we consider the independent variable as time). In particular, let  $y = \frac{1}{\sigma^2}x + c$  and  $u(x) = v(y)$ , then substituting to (1.1) we find

$$-{}_1\mathcal{Q}_x^{1/2}u(x) = \sigma -{}_a\mathcal{Q}_y^{1/2}v(y). \quad (\text{B.10})$$

Investigating the singular values of the operator suggests that as  $\sigma \rightarrow 0$  it is only a single singular value that decays to zero and that it might be possible to regularise the problem. However, this is beyond the scope of the current paper and we avoid this limiting case for now.

## REFERENCES

- [1] J. ABDALKHANI, *A numerical approach to the solution of Abel integral equations of the second kind with nonsmooth solution*, Journal of Computational and Applied Mathematics, 29 (1990), pp. 249–255.
- [2] B. K. ALPERT AND V. ROKHLIN, *A fast algorithm for the evaluation of Legendre expansions*, SIAM Journal on Scientific and Statistical Computing, 12 (1991), pp. 158–179.
- [3] G. E. ANDREWS, R. ASKEY, AND R. ROY, *Special functions*, vol. 71, Cambridge University Press, 1999.
- [4] J. L. AURENTZ AND L. N. TREFETHEN, *Chopping a Chebyshev series (submitted)*, 2015.
- [5] R. L. BAGLEY AND P. J. TORVIK, *Fractional calculus – a different approach to the analysis of viscoelastically damped structures*, 1983.
- [6] ———, *On the appearance of the fractional derivative in the behavior of real materials*, 1984.
- [7] E. G. BAJLEKOVA, *Fractional evolution equations in Banach spaces*, ProQuest LLC, Ann Arbor, MI, 2001. Thesis (Dr.)—Technische Universiteit Eindhoven (The Netherlands).
- [8] S. CHEN, J. SHEN, AND L.-L. WANG, *Generalized Jacobi functions and their applications to fractional differential equations*, Math. Comp., 85 (2016), pp. 1603–1638.
- [9] O. CHRISTENSEN, *An Introduction to Frames and Riesz Bases*, Birkhauser, 2003.
- [10] M. CUI, *Compact finite difference method for the fractional diffusion equation*, Journal of Computational Physics, 228 (2009), pp. 7792–7804.
- [11] M. DALIR AND M. BASHOUR, *Applications of fractional calculus*, Applied Mathematical Sciences, 4 (2010), pp. 1021–1032.
- [12] W. DENG, *Finite element method for the space and time fractional Fokker–Planck equation*, SIAM Journal on Numerical Analysis, 47 (2008), pp. 204–226.
- [13] *NIST Digital Library of Mathematical Functions*. <http://dlmf.nist.gov/>, Release 1.0.10 of 2015-08-07. Online companion to [25].
- [14] T. A. DRISCOLL, N. HALE, AND L. N. TREFETHEN, *Chebfun Guide*, Pafnuty Publications, 2014.
- [15] N. FORD, J. XIAO, AND Y. YAN, *A finite element method for time fractional partial differential equations*, Fractional Calculus and Applied Analysis, 14 (2011), pp. 454–474.
- [16] N. HALE, *Companion code to this paper*. [https://github.com/nickhale/fracspect\\_code](https://github.com/nickhale/fracspect_code). Last accessed 17 Oct 2016.
- [17] N. HALE AND A. TOWNSEND, *A fast, simple, and stable Chebyshev–Legendre transform using an asymptotic formula*, SIAM J. Sci. Comput., 36 (2014), pp. A148–A167.
- [18] R. HILFER, *Applications of fractional calculus in physics*, World Scientific, 2000.
- [19] X. LI AND C. XU, *A space-time spectral method for the time fractional diffusion equation*, SIAM J. Numer. Anal., 47(3) (2009), p. 2108–2131.
- [20] F. LIU, V. ANH, AND I. TURNER, *Numerical solution of the space fractional Fokker–Planck equation*, Journal of Computational and Applied Mathematics, 166 (2004), pp. 209–219.
- [21] R. L. MAGIN, *Fractional calculus in bioengineering*, Begell House Redding, 2006.
- [22] ———, *Fractional calculus models of complex dynamics in biological tissues*, Computers & Mathematics with Applications, 59 (2010), pp. 1586–1593.
- [23] M. M. MEERSCHAERT AND C. TADJERAN, *Finite difference approximations for two-sided space-fractional partial differential equations*, Applied numerical mathematics, 56 (2006), pp. 80–90.
- [24] K. B. OLDHAM, *Fractional differential equations in electrochemistry*, Advances in Engineering Software, 41 (2010), pp. 9–12.
- [25] F. W. J. OLVER, D. W. LOZIER, R. F. BOISVERT, AND C. W. CLARK, eds., *NIST Handbook of Mathematical Functions*, Cambridge University Press, New York, NY, 2010. Print companion to [13].
- [26] S. OLVER, *ApproxFun.jl v0.2*, <https://github.com/approxfun/approxfun.jl>.
- [27] S. OLVER AND A. TOWNSEND, *A fast and well-conditioned spectral method*, SIAM Rev., 55 (2013), pp. 462–489.
- [28] S. OLVER AND A. TOWNSEND, *A practical framework for infinite-dimensional linear algebra*, in Proceedings of the 1st First Workshop for High Performance Technical Computing in Dynamic Languages, 2014, pp. 57–62.
- [29] M. D. ORTIGUEIRA AND J. T. MACHADO, *Fractional calculus applications in signals and systems*, Signal Processing, 86 (2006), pp. 2503 – 2504. Special Section: Fractional Calculus Applications in Signals and Systems.
- [30] M. RIESZ, *L’intégrale de Riemann–Liouville et le problème de Cauchy*, Acta Math., 81 (1949), pp. 1–223.
- [31] J. SABATIER, O. P. AGRAWAL, AND J. T. MACHADO, *Advances in fractional calculus*, vol. 4, Springer, 2007.
- [32] E. SCALAS, R. GORENFLO, AND F. MAINARDI, *Fractional calculus and continuous-time finance*, Physica A: Statistical Mechanics and its Applications, 284 (2000), pp. 376–384.
- [33] H. SHENG, Y. CHEN, AND T. QIU, *Fractional processes and fractional-order signal processing: techniques and applications*, Springer Science & Business Media, 2011.



- [34] R. M. SLEVINSKY AND S. OLVER, *A fast and well-conditioned spectral method for singular integral equations*, preprint, (2015).
- [35] G. W. STEWART, *Afternotes goes to graduate school*, Society for Industrial and Applied Mathematics (SIAM), Philadelphia, PA, 1998. Lectures on advanced numerical analysis.
- [36] A. TOWNSEND AND S. OLVER, *The automatic solution of partial differential equations using a global spectral method*, J. Comput. Phys., 299 (2015), pp. 106–123.
- [37] A. TOWNSEND, M. WEBB, AND S. OLVER, *Fast polynomial transforms based on Toeplitz and Hankel matrices*, 2016. (submitted).
- [38] G. M. VASIL, K. J. BURNS, D. LECOANET, S. OLVER, B. P. BROWN, AND J. S. OISHI, *Tensor calculus in polar coordinates using Jacobi polynomials*, J. Comp. Phys., (2016). To appear.
- [39] T. G. WRIGHT., *Eigtool*, 2002.
- [40] S. B. YUSTE AND L. ACEDO, *An explicit finite difference method and a new von Neumann-type stability analysis for fractional diffusion equations*, SIAM Journal on Numerical Analysis, 42 (2005), pp. 1862–1874.
- [41] M. ZAYERNOURI AND G. E. KARNIADAKIS, *Fractional spectral collocation method*, SIAM J. Sci. Comput., 36 (2014), pp. A40–A62.
- [42] L. ZHAO, W. DENG, AND J. S. HESTHAVEN, *Spectral methods for tempered fractional differential equations*, ArXiv e-print: 1603.06511, (2016).